

Overparameterized Linear Regression under Adversarial Attacks

Antônio H. Ribeiro and Thomas B. Schön

Abstract—As machine learning models start to be used in critical applications, their vulnerabilities and brittleness become a pressing concern. Adversarial attacks are a popular framework for studying these vulnerabilities. In this work, we study the error of linear regression in the face of adversarial attacks. We provide bounds of the error in terms of the traditional risk and the parameter norm and show how these bounds can be leveraged and make it possible to use analysis from non-adversarial setups to study the adversarial risk. The usefulness of these results is illustrated by shedding light on whether or not overparameterized linear models can be adversarially robust. We show that adding features to linear models might be either a source of additional robustness or brittleness. We show that these differences appear due to scaling and how the ℓ_1 and ℓ_2 norms of random projections concentrate. We also show how the reformulation we propose allows for solving adversarial training as a convex optimization problem. This is then used as a tool to study how adversarial training and other regularization methods might affect the robustness of the estimated models.

I. INTRODUCTION

The seminal work by Belkin *et al.* [1] has shown an interesting line of reasoning that help explain how very rich models such as neural networks that are trained to exactly fit the data can still generalize well into new datapoints. Indeed increasing the model size has been a standard strategy in obtaining better models of this type and one of the big mysteries behind them [2]. The so-called *double-descent* phenomenon [1] provides insight into this observation and shows that as we increase the model flexibility, it is possible to reach a point where the training error is zero. If we continue to increase the model complexity beyond this point, the model can eventually start to generalize well again.

The explanation is that larger models can fit the training dataset with smoother solutions and hence generalize better in the test. Smoothness is naturally related to robustness. The idea that increasing the model size can be a recipe to obtain more robust models has indeed recently been developed by Bubeck *et al.* [3] using isoperimetric inequalities.

In another line of work, adversarial examples have provided a useful setting when it comes to studying robustness. They consider inputs contaminated with small disturbances chosen to maximize the model error when compared to the initial and correct prediction. The susceptibility of state-of-the-art neural network models to very small input modifications [4] gave the framework a lot of attention from the research community. Initial speculation that the highly nonlinear nature of deep neural networks was the cause of its vulnerabilities to attacks [4]

The authors are with the Department of Information Technology, Uppsala University, Sweden (emails: antonio.horta.ribeiro@it.uu.se, thomas.schon@it.uu.se)

was later dismissed. Indeed, Goodfellow *et al.* [5] shows that the existence of vulnerabilities to adversarial attacks can be explained and observed in a purely linear setting and the high dimensionality is pointed out as a main cause of the problem.

This somewhat conflicting view of the relation between high dimensionality and model robustness served as the driving force for this work. High-dimensionality is both seen as a source of brittleness and as a potential recipe for producing robust models. Indeed, linear models are a natural setup to study and understand these ideas: not only can they be made vulnerable to adversarial attacks, but the double-descent phenomenon can also be observed in a purely linear setting [6], [7]. Here we show how both views can be reconciled and how each behavior can be observed (see Figure 1).

Contributions

This paper makes the following contributions:

- 1) We show that **the analysis of adversarial attacks can be significantly simplified in linear regression problems**. This is developed in Section III, where we show how to reformulate the expression of the adversarial risk, and in Section IV, where we obtain bounds that allow for reusing the analysis from other setups in adversarial scenarios.
- 2) The minimum-norm solution is commonly used to select overparameterized models in connection to the study of the double-descent phenomenon [1], [6]. In Section IV, we study the adversarial robustness of the minimum-norm solution.
 - a) We use asymptotic and non-asymptotic analysis to explain when we can observe **double-descent in adversarial scenarios**.
 - b) We show how overparameterized models tend to become **smoother** in the ℓ_2 norm, but not in the ℓ_1 norm. It is also shown how this can be used to explain when more features make the model more **vulnerable to some types of adversarial attacks**.
- 3) **Adversarial training** is a standard method to produce models that are robust to adversarial attacks [8]. In Section V, we show how adversarial training affects the conclusion obtained for minimum-norm solution models.
 - a) We show how our formulation allows for solving adversarial training in linear regression as a **convex optimization** problem.
 - b) We show how adversarial training affects the way robustness changes with the number of features. An illustration of cases when it is effective and when it is not is also provided.
 - c) We compare and establish similarities with **ridge regression** and **lasso** [9].

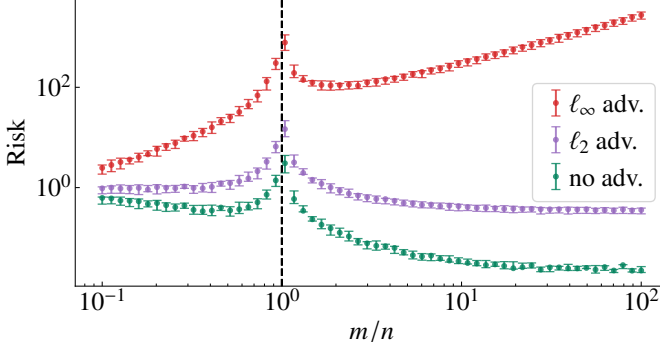


Fig. 1: **Double-descent vs robustness-accuracy trade-off.** On the x -axis we have the ratio between the number of features m and the number of training datapoints n . The model traditional risk (no adv.) continually decreases in the overparameterized region, achieving significantly better results than in the underparameterized region. On the other hand, increasing the number of features continuously produce worse adversarial robustness for the risk of ℓ_∞ adversarial attacks. For an ℓ_2 adversary, however, the model actually benefits from operating in the overparameterized region and larger models yield better adversarial robustness. The precise setup for this example is provided in Section IV-G.

Related work

The study of adversarial attacks pre-dates the widespread use of deep neural networks [10], [11]. An overview of earlier work is provided by Biggio *et al.* [12]. Nonetheless, the susceptibility of high-performance neural networks gave this framework higher visibility [4]. The conflict between robustness and high-performance models is explored by Tsipras *et al.* [13] and Ilyas *et al.* [14]. Indeed, one of the examples we give for the worst-case scenario of the ℓ_∞ adversarial error is motivated by an idea presented in [13]. Moreover, simple examples where high-dimensional inputs yield easy-to-construct adversarial examples are abundant in the literature [15]. Also close to our work is that from Yin *et al.* [16], which provides an analysis of ℓ_∞ attack on linear classifiers based on the Rademacher complexity. They showed an unavoidable dimension dependence, unless the weight vector has a bounded ℓ_1 norm.

The analysis of the robustness of more general nonlinear models, such as neural networks is provided in [17] and extended in Bubeck *et al.* [3]. They show how overparameterization can be a recipe for robustness. An alternative view is provided in [18], [19], where it is shown that ReLU neural networks can be made vulnerable since what these models learn is locally very similar to random linear functions. As we mentioned in the introduction, our work tries to reconcile these somewhat conflicting views in the context of linear models.

The double-descent performance curve has been experimentally observed for a variety of machine learning models, such as random Fourier features, random forest, shallow networks, transformers and convolutional network and nonlinear ARX models; and for datasets obtained in diverse context, including image classification, natural language processing datasets and the identification of nonlinear dynamical systems [1], [20]–[23].

Theoretical models for such phenomena are also often pursued: Bartlett *et al.* [6] derive non-asymptotic bounds for linear regression models using concentration inequalities. In [21] the authors draw connections with the physical phenomena of "jamming" in a class of glassy systems. Deng *et al.* [24] characterize logistic regression test error using the Gaussian min-max theorem. Muthukumar *et al.* [25] provides bounds on the risk.

Random matrix theory has been a useful tool for studying statistical phenomenon. The framework and its potential for explaining and studying neural networks have been the focus of recent work [28]–[30]. It has also been a powerful tool in producing theoretical models for the double-descent phenomenon [7], [27], [31]–[33]. In our study of linear regression with random covariates, we make direct use of the asymptotic results obtained by Hastie *et al.* [7].

Theoretical analysis of models under adversarial attacks is currently a rather popular topic. D'Amour *et al.* [26] provide asymptotics based on Mei *et al.* [27]. They take a different approach than us and study scenarios where the adversarial attack is constrained to not change the risk. The theoretical model is used to explain how underspecification might present a challenge in deployment, and is backed by experiments. Under additional assumptions, it is generally possible to obtain sharper bounds than ours [34], [35]. Moreover, there is a plethora of work developing exact asymptotics to the adversarial risk and for adversarially trained models. Taheri *et al.* [36] derived asymptotics for adversarial training in binary classification. Moreover, Javanmard *et al.* [37] provide asymptotics for adversarial attacks in linear regression. Javanmard *et al.* [38] study it in classification settings and Hassani *et al.* [39] obtain exact asymptotics for random feature regressions.

These asymptotics are often used to gain insight into the effect of adversarial training and adversarial robustness. Javanmard *et al.* [37] use it to study the trade-off between adversarial risk and standard risk using the parameter of the adversarial training to control the trade-off between these two. Javanmard *et al.* [38] studies how overparameterization affects robustness to perturbations in the input and Min *et al.* [40] studies how the size of the dataset affects adversarial performance. Interestingly, while they take a very different route, our results are consistent with theirs, and here we can observe cases where the adversarial performance degrades as the size of the dataset increases.

The derivation of exact asymptotics is an impressive technical development, however, we point out that it is not always trivial to gain insight from these results. The asymptotics obtained often do not have closed-form expressions and require the solution of either polynomials or integral equations. Here, we advocate a simpler approach: approximating the adversarial risk using terms that often appear in other contexts. We believe that this is a powerful tool to gain insight into the problem, providing extra flexibility for quickly navigating between different setups.

II. PROBLEM FORMULATION

Consider a training dataset $\mathcal{S} = \{(x_i, y_i)\}_{i=1}^n$ consisting of n i.i.d. datapoints of dimension $\mathbb{R}^m \times \mathbb{R}$, sampled from the

distribution $(x_i, y_i) \sim P_{x,y}$. To this data, we fit a *linear model* from the function class $\{\tilde{\beta}^\top x \mid \tilde{\beta} \in \mathbb{R}^m\}$. We use $\hat{\beta}$ to denote the parameter estimated from the training data. The estimation method is detailed in what follows.

We will use subscripts to denote the source of randomness considered in the conditional expectation. For instance, let x, y, z, w be random variables, we use $\mathbb{E}_{x,y}[f(x, y, z, w)]$ to denote the expectation with respect to x, y and conditioned on the variables that are not explicitly mentioned in the subscript, here z and w .

Let $(x_0, y_0) \sim P_{x,y}$ be a point not seen during training and independently sampled from the same distribution as the rest of the data. We denote the out-of-sample *prediction risk* by

$$R(\hat{\beta}) = \mathbb{E}_{x_0, y_0} [(y_0 - x_0^\top \hat{\beta})^2]. \quad (1)$$

The ℓ_p *adversarial risk* is defined as

$$R_p^{\text{adv}}(\hat{\beta}) = \mathbb{E}_{x_0, y_0} \left[\max_{\|\Delta x_0\|_p \leq \delta} (y_0 - (x_0 + \Delta x_0)^\top \hat{\beta})^2 \right], \quad (2)$$

which is the risk when the model is subject to a disturbance Δx_0 that results in the worst possible performance inside the region $\|\Delta x_0\|_p \leq \delta$. Here, we use $\|\cdot\|_p$ to denote the ℓ_p norm of a vector, i.e.,

Definition 1 (Vector p -norms). *Let $a \in \mathbb{R}^n$ and $p \in \mathbb{R}$, $p \geq 1$, then the p -norm of this vector is defined as*

$$\|a\|_p = \left(\sum_{i=1}^n |a_i|^p \right)^{\frac{1}{p}}, \quad (3)$$

with $\|a\|_\infty = \max_{1 \leq i \leq n} |a_i|$.

Moreover, the *empirical risk* is denoted by

$$\hat{R}(\hat{\beta}) = \frac{1}{n} \sum_{i=1}^n (y_i - x_i^\top \hat{\beta})^2, \quad (4)$$

where the expectation w.r.t. the true distribution is replaced by the average over the observed training samples. We use a similar notation for the *empirical adversarial risk*, $\hat{R}_p^{\text{adv}}(\hat{\beta})$.

III. ADVERSARIAL RISK IN LINEAR REGRESSION

In this paper, we show that the adversarial risk for linear regression can be simplified. The following lemma gives a quadratic form for the adversarial risk defined in Eq. (2).

Lemma 2. *Let q be a positive real number for which $\frac{1}{p} + \frac{1}{q} = 1$, then¹*

$$R_p^{\text{adv}}(\hat{\beta}) = \mathbb{E}_{x_0, y_0} \left[(|y_0 - x_0^\top \hat{\beta}| + \delta \|\hat{\beta}\|_q)^2 \right]. \quad (5)$$

The lemma is simple, but it turns out to be a useful tool when analysing robustness to adversarial attacks and adversarial training. A contribution of this paper is to show how it can be used in various situations. In Section IV, Lemma 2 is used to analyse the adversarial robustness of linear models and the interplay between overparameterization and robustness. In

¹The result still holds for the pair of values $(p = 1, q = \infty)$ and $(p = \infty, q = 1)$.

Section V, we show how the formula allows for an efficient method for adversarial training using convex programming.

The proof of the lemma is based on Hölder's inequality $|\beta^\top \Delta x| \leq \|\beta\|_p \|\Delta x\|_q$ and on the fact that we can, given β , construct Δx such that the equality holds. The next proposition gives the precise construction that we will make use of.

Proposition 3. *Given $p, q \in (1, \infty)$ such that $1/p + 1/q = 1$ and $\beta \in \mathbb{R}^m$, $\Delta x \in \mathbb{R}^m$. We have $|\beta^\top \Delta x| = \|\beta\|_p \|\Delta x\|_q$ when the i -th component is $\Delta x_i = |\beta_i|^{q/p}$. Moreover, if $\Delta x_i = \text{sign}(\beta_i)$ for every i , then $|\beta^\top \Delta x| = \|\beta\|_1 \|\Delta x\|_\infty$. If*

$$\Delta x_i = \frac{s_i}{\sum_i s_i} \quad \text{for} \quad s_i = \begin{cases} 1 & \text{if } \beta_i = \max_i \beta_i \\ 0 & \text{otherwise} \end{cases}$$

then $|\beta^\top \Delta x| = \|\beta\|_\infty \|\Delta x\|_1$.

The above proposition is well-known. Indeed, most adversarial attacks are constructed based on it. For instance, the Fast Gradient Sign Method (FGSM) [5] linearizes the neural network and applies the above construction for $p = \infty$ to obtain the adversarial perturbation. We are now ready to prove Lemma 2.

Proof of Lemma 2. For $1 \leq p \leq \infty$, let q be a positive real number such that $\frac{1}{p} + \frac{1}{q} = 1$. Let $e_0 = y_0 - x_0^\top \hat{\beta}$. The adversarial risk (2) can, after some algebraic manipulation, be rewritten as

$$R_p^{\text{adv}}(\hat{\beta}) = \mathbb{E}_{x_0, y_0} \left[e_0^2 + \max_{\|\Delta x_0\|_p \leq \delta} ((\Delta x_0^\top \hat{\beta})^2 - 2e_0 \Delta x_0^\top \hat{\beta}) \right].$$

In turn, if we let $r = \Delta x_0^\top \hat{\beta}$ since $\|\Delta x_0\|_p \leq \delta$, Hölder's inequality yields $|r| \leq \delta \|\hat{\beta}\|_q$, for q satisfying $1/p + 1/q = 1$. Since Proposition 3 guarantees that we can always choose vectors such that the equality holds, the term inside the expectation of the right-hand side is equal to:

$$M = \max_{|r| \leq \delta \|\hat{\beta}\|_q} (r^2 - 2e_0 r).$$

Now the maximum is attained at $r = -\delta \|\hat{\beta}\|_q$ if $e_0 \geq 0$ and at $r = \delta \|\hat{\beta}\|_q$ if $e_0 < 0$, hence $M = \delta^2 \|\hat{\beta}\|_q^2 + 2\delta \|\hat{\beta}\|_q |e_0| + |e_0|^2$.

$$R_p^{\text{adv}}(\hat{\beta}) = \mathbb{E}_{x_0, y_0} \left[\delta^2 \|\hat{\beta}\|_q^2 + 2\delta \|\hat{\beta}\|_q |e_0| + |e_0|^2 \right]. \quad (6)$$

□

IV. ADVERSARIAL ROBUSTNESS OF LINEAR MODELS

Lemma 2 provides an easy to analyse formula for the adversarial risk. By expanding the square and using the linearity of the expectation we obtain:

$$R_p^{\text{adv}}(\hat{\beta}) = \delta^2 \|\hat{\beta}\|_q^2 + 2\delta \|\hat{\beta}\|_q \mathbb{E}_{x_0, y_0} [y_0 - x_0^\top \hat{\beta}] + R(\hat{\beta}). \quad (7)$$

An approximation of Eq. (7) can be obtained by simply dropping the middle term on the right-hand side

$$R_p^{\text{adv}}(\hat{\beta}) \approx R(\hat{\beta}) + \delta^2 \|\hat{\beta}\|_q^2. \quad (8)$$

We will formalize the notion later. However, for now, we just highlight that this approximation makes the similarity between the adversarial risk and other loss functions used in more traditional regularized regression settings explicit. We

can naturally see similarities with lasso for $q = 1$ and with ridge regression for $q = 2$.

The approximation is also a useful simplification since it allows for the analysis of adversarial robustness from values that are often obtained from other analysis (the traditional risk and the parameter norm). For instance, from the double-descent literature, it is well-known that the ℓ_2 -norm of the estimated parameter often also exhibits a double-descent behavior as a function of the number of features. This is observed experimentally, for instance, by Belkin *et al.* [1]. Hence, the above approximation gives an easy way to understand why we can expect double-descent behavior for the ℓ_2 adversarial risk. The approximation is also enough to justify the potential brittleness of high-dimensional models. The next example demonstrates a fairly simple case where such behavior can be observed.

A. Motivating example: weak features

In this section, we show brittleness and vulnerability to ℓ_∞ adversarial attacks arising from high dimensionality. Tsipras *et al.* [13] makes use of a linear example to motivate their argument that robustness and accuracy might be at odds. We show a modified construction² to motivate how brittleness might appear in linear examples. The construction makes use of many features that are weakly correlated with the output. Let the input $x = (x^1, \dots, x^m)$ and the output y be normally distributed:

$$y \sim \mathcal{N}(0, 1) \text{ and } x^j \mid y \sim \mathcal{N}\left(\frac{y}{\eta}, \frac{1}{\eta}\right) \text{ for } j = 1, \dots, m. \quad (9)$$

Following the choice of Tsipras *et al.* [13], we use $\eta = \frac{1}{\sqrt{m}}$ so that $\mathbb{E}_x[\|x\|_2]$ remains constant with the number of features. Here, we can show that the optimal predictor $\hat{\beta} = \left[\frac{1}{\sqrt{m}}, \dots, \frac{1}{\sqrt{m}}\right]$ results in a prediction $\hat{y} = \hat{\beta}^\top x$ that follows the distributions $(\hat{\beta}^\top x) \mid y \sim \mathcal{N}(y, \frac{1}{m})$. This means that the prediction risk of this model is $R(\hat{\beta}) = \mathbb{E}_{x,y}[(y - \hat{\beta}^\top x)^2] = \frac{1}{m}$. Hence, the risk of our predictor goes to zero $R \rightarrow 0$ as the number of features goes to infinity, $m \rightarrow \infty$.

Here, $\|\hat{\beta}\|_1 = \sqrt{m}$, implying that the ℓ_∞ adversarial risk would grow with a rate $\Omega(m)$ by Eq. (8). This is one example where the traditional risk goes to zero with the number of features *at the same time* as the ℓ_∞ adversarial risk grows indefinitely.

There are two aspects of this example that we will further refine in the coming sections. The first is that we are using an estimator that is obtained by minimizing the true risk, which is not a procedure that can be used in practice. In what follows, we show that a similar effect can be obtained if the empirical risk is minimized. The second aspect is the scaling η , we will motivate different choices and show how they can yield quite different results.

²The construction is quite similar. The only differences are: 1) it is a regression problem rather than a classification problem; and, 2) we use y/η rather than y as the conditional mean of x^j (in Eq. (9)). This is done to ensure that the signal-to-noise ratio is constant with η .

B. Preliminaries

Here we focus the minimum norm solution, which is often used when studying the behavior of overparameterized models in connection with the double-descent phenomenon [1]. In our analysis, we will formalize the notion conveyed by the approximation in Eq. (8), using the upper and lower bounds

$$R(\hat{\beta}) + \delta^2 \|\hat{\beta}\|_q^2 \leq R_p^{\text{adv}}(\hat{\beta}) \leq \left(\sqrt{R(\hat{\beta})} + \delta \|\hat{\beta}\|_q \right)^2, \quad (10)$$

which follow directly from Lemma 2. We will assume that the training and test data have been generated linearly with additive noise:

$$(x_i, \epsilon_i) \sim P_x \times P_\epsilon, \quad y_i = x_i^\top \beta + \epsilon_i, \quad (11)$$

where P_ϵ is a distribution in \mathbb{R} such that $\mathbb{E}[\epsilon_i] = 0$ and $\mathbb{V}[\epsilon_i] = \sigma^2$ and ϵ_i is assumed to be independent of x_i . Moreover, $\mathbb{E}[x_i] = 0$ and $\text{Cov}[x_i] = \Sigma$. The ℓ_2 norm of the data generation parameter is denoted by $\|\beta\|_2^2 = r^2$.

Let $X \in \mathbb{R}^{n \times m}$ denote the matrix consisting of stacked training inputs x_i^\top and similarly let $y \in \mathbb{R}^n$ denote the output vector. The parameters are estimated as

$$\hat{\beta} = (X^\top X)^\dagger X^\top y, \quad (12)$$

where $(X^\top X)^\dagger$ represents the pseudo-inverse of $X^\top X$. In the underparameterized ($m < n$) region, it corresponds to the least-square solution. In the overparameterized ($m > n$) case, when more than one solution is possible, this corresponds to the solution for which the parameter norm $\|\hat{\beta}\|_2$ is minimum, the **minimum-norm solution**.

From Eq. (11) and Eq. (12) it follows that:

$$\hat{\beta} = \underbrace{(X^\top X)^\dagger X^\top X \beta}_{\Phi} + \underbrace{(X^\top X)^\dagger X^\top \epsilon}_{n\hat{\Sigma}^\dagger}, \quad (13)$$

where we denote $\hat{\Sigma} = \frac{1}{n} X^\top X$, $\Phi = \hat{\Sigma}^\dagger \hat{\Sigma}$ and $\Pi = I - \Phi$. Here, Φ and Π are orthogonal projectors: Π is the projection into the null space and Φ into the row space of X . The first term in Eq. (13) can be understood as a projection of the original parameter into the row space of the regressors and it is the parameters estimated in a noiseless scenario. The second term is the consequence of the noise. It follows from it, that the risk and the expected parameter norm can be decomposed as in the next Lemma. The proof is provided in the Supplementary Material.

Lemma 4 (Bias-variance decomposition). *Denote $\|z\|_\Sigma^2 = z^\top \Sigma z$. The expected risk and ℓ_2 parameter norm are*

$$\mathbb{E}_\epsilon[R(\beta)] = \|\Pi\beta\|_\Sigma^2 + \frac{\sigma^2}{n} \text{tr}(\hat{\Sigma}^\dagger \Sigma) + \sigma^2, \quad (14)$$

$$\mathbb{E}_\epsilon[\|\hat{\beta}\|_2^2] = \|\Phi\beta\|_2^2 + \frac{\sigma^2}{n} \text{tr}(\hat{\Sigma}^\dagger). \quad (15)$$

The following bounds can be used in conjunction with Lemma 4 to analyze the adversarial risk

$$R + \delta^2 L_q \leq R_p^{\text{adv}} \leq \left(\sqrt{R} + \delta \sqrt{L_q} \right)^2, \quad (16)$$

where $L_q = \mathbb{E}_\epsilon[\|\hat{\beta}\|_q^2]$, $R = \mathbb{E}_\epsilon[R(\hat{\beta})]$ and $R_p^{\text{adv}} = \mathbb{E}_\epsilon[R_p^{\text{adv}}(\hat{\beta})]$.

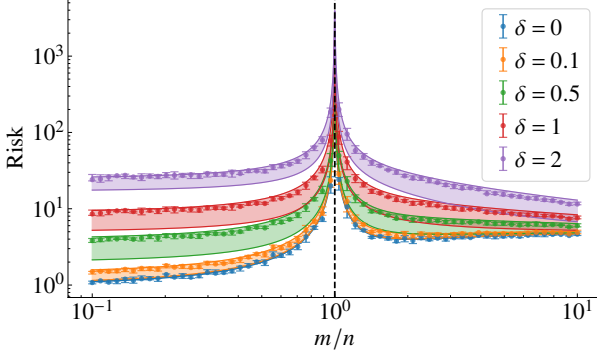


Fig. 2: **Adversarial ℓ_2 risk, isotropic features.** The solid line shows the upper and lower bounds on the asymptotic risk. The results are for isotropic features with $r^2 = 2$, $\sigma^2 = 1$. The error bars give the median and the 0.25 and 0.75 quantiles obtained from numerical experiments (10 realizations) with a fixed training dataset of size $n = 300$.

C. Isotropic feature model

Here, we analyse the case of isotropic features, i.e. we assume that the input x_i has mean zero and unit variance ($\Sigma = I_m$). For this case, results from random matrix theory can be used to establish asymptotics for the terms in Eqs. (14) and (15).

Lemma 5 (Isotropic features, Hastie *et al.* [7]). *For isotropic features with a moment of order greater than 4 that is finite. As $m, n \rightarrow \infty$, $m/n \rightarrow \gamma$, almost surely*

$$\mathbb{E}_\epsilon [R(\hat{\beta})] \rightarrow \begin{cases} \sigma^2 \frac{\gamma}{1-\gamma} + \sigma^2 & \gamma < 1, \\ r^2(1 - \frac{1}{\gamma}) + \sigma^2 \frac{1}{\gamma-1} + \sigma^2 & \gamma > 1, \end{cases} \quad (17)$$

$$\mathbb{E}_\epsilon [\|\hat{\beta}\|_2^2] \rightarrow \begin{cases} r^2 + \sigma^2 \frac{\gamma}{1-\gamma} & \gamma < 1, \\ r^2 \frac{1}{\gamma} + \sigma^2 \frac{1}{\gamma-1} & \gamma > 1. \end{cases} \quad (18)$$

Both terms do have an asymptotic behavior that depends on the ratio γ between the number of features (m) and the number of training datapoints (n). In Figure 2, we illustrate one example of how the bounds in (16) can be combined with the asymptotic results above to obtain asymptotic lower and upper bounds. The results obtained from the experiments closely follow these asymptotic bounds.

Let us already now informally point out that the second part of Lemma 5 states that for a sufficiently large problem, in the overparameterized region,

$$\|\hat{\beta}\|_2^2 \approx \left(r^2 \frac{1}{m/n} + \sigma^2 \frac{1}{m/n - 1} \right). \quad (19)$$

We formalize the notion in Section IV-D using concentration of measure. It follows from it that even for a fixed signal magnitude, the norm of the estimated parameter decays with the number of parameters for overparameterized problems, i.e., $\|\hat{\beta}\|_2 = \mathcal{O}\left(\left(\frac{m}{n}\right)^{-\frac{1}{2}}\right)$. The model becomes ‘smoother’ as more parameters are added to the model. This naturally yields models more robust to ℓ_2 perturbations. This can be observed in Figure 2: after the local minima $\gamma = \frac{r}{r+\sigma}$ in the standard risk, the risk is increasing with γ . However, the adversarial

risk for, say, $\delta = 2$ is decreasing due to the tendency of the minimum-norm solution to select smoother solutions. Moreover, while the standard risk does not have better results in the overparameterized region than in the underparameterized region, the adversarial risk in the overparameterized region can actually be better than the adversarial risk in the underparameterized region.

D. Non-asymptotic results for the parameter ℓ_2 norm

Central to our analysis of ℓ_2 adversarial attacks is the idea that the parameter norm decays with the rate $\mathcal{O}\left(\left(\frac{m}{n}\right)^{-\frac{1}{2}}\right)$ even when the data generator parameter remain constant, i.e. $\|\beta\|_2 = r$. The next theorem formalizes this intuition. We do not attempt to provide the most general result, instead, our choice of formulation is motivated by the fact that many of the steps in proving this theorem can be carried on to the ℓ_1 norm, as we will discuss later.

Theorem 6. *Let the data be generated according to Eq. (11). Assume additionally that $m > n$ and:*

- 1) *The noise ϵ and the regressors x are sub-Gaussian.*
- 2) *the regressor vector x is sampled from a rotationally invariant distribution.*

Then there exists constants $c, C > 0$ such that for all $t < \sqrt{\frac{m}{n}}$ with probability $1 - 2 \exp(-ct^2n)$ we have:

$$\|\hat{\beta}\|_2 \leq r \frac{1+t}{\sqrt{m/n}} + \sigma \frac{1+t}{C \sqrt{m/n} - 1}.$$

This theorem provides a non-asymptotic result and an exponential rate of convergence. It strengthens the assumptions from the previous section in two ways. First, it assumes the variables are sub-Gaussian, which is used to obtain an exponential rate of convergence. If this assumption is relaxed lower rates of concentration are obtained. For instance, Hastie *et al.* [7] does not assume this, which results in a convergence rate of $n^{-1/7}$.

Secondly, it assumes the regressor vector to be rotationally invariant. That is, given an orthogonal matrix Q , multiplication by this matrix does not alter the distribution of the original vectors, i.e. $x \sim Qx$. Standard examples where x is rotationally invariant are values sampled from standard Gaussian or from the uniform distribution over the sphere. Rotational invariance implies isotropy but not all isotropic distributions are rotationally invariant. Hence, this is again a stronger assumption.

From Lemma 4 we have:

$$\mathbb{E}_\epsilon [\|\hat{\beta}\|_2^2] = \|\Phi\beta\|_2^2 + \frac{\sigma^2}{n} \text{tr}(\hat{\Sigma}^\dagger).$$

The next Lemma gives concentration inequalities for the eigenvalues of $\hat{\Sigma}^\dagger$. If we use $\lambda_i(\hat{\Sigma}^\dagger)$ to denote the i -th eigenvalue of $\hat{\Sigma}^\dagger$, we have that $\text{tr}(\hat{\Sigma}^\dagger) = \frac{1}{n} \sum_i \lambda_i(\hat{\Sigma}^\dagger)$. Hence, the following result immediately implies that the second term of the above expression concentrates around $\Theta\left(\left(\frac{m}{n}\right)^{-1}\right)$. The proof is provided in the Supplementary Material.

Lemma 7. *Let $x_i \in \mathbb{R}^m$ be independently sampled sub-Gaussian random vectors, $\hat{\Sigma} = \frac{1}{n} \sum_{i=1}^n x_i x_i^\top$, and let $m > n$.*

Then there exist a constant $C > 0$ such that, with probability greater than $1 - 2 \exp(-m)$,

$$\frac{1}{(C\sqrt{\frac{m}{n}} + 1)^2} \leq \lambda_i(\hat{\Sigma}^\dagger) \leq \frac{1}{(C\sqrt{\frac{m}{n}} - 1)^2}.$$

Next, we turn to the analysis of the first term in Eq. (15). In the case $m > n$, Φ is a projection matrix that projects a vector from \mathbb{R}^m into a subspace of dimension n . The set of all possible subspaces of dimension n in \mathbb{R}^m is well studied and known as the Grassmannian manifold $G(m, n)$. There is a one-to-one relationship between the projection matrices Φ and the points in this manifold. For the case when X is rotationally invariant, we have, given any orthogonal matrix Q that

$$\Phi = (X^\top X)^\dagger (X^\top X) \sim Q(X^\top X)^\dagger (X^\top X) Q^\top = Q \Phi Q^\top.$$

Hence, the subspace is invariant to rotation and it is possible to establish that the matrix Φ is a random projection that projects into a subspace sampled uniformly (i.e., Haar measure) from the Grassmannian $G(m, n)$. The next result is from [41, Lemma 5.3.2] and it states that the norm $\|\Phi\beta\|_2$ of the projection of β into this n dimensional subspace concentrates around $\sqrt{\frac{n}{m}}\|\beta\|_2$.

Lemma 8 (Vershynin [41, Lemma 5.3.2]). *Let $\beta \in \mathbb{R}^m$ be a vector and $\Phi \in \mathbb{R}^{m \times m}$ be a projection from \mathbb{R}^m onto a random n -dimensional subspace uniformly sampled from $G(m, n)$. Then,*

- 1) $\mathbb{E}_\Phi [\|\Phi\beta\|_2^2] = \frac{n}{m}\|\beta\|_2^2$;
- 2) *There exist a constant c , such that with probability greater than $1 - 2 \exp(-ct^2n)$, we have:*

$$(1-t)\sqrt{\frac{n}{m}}\|\beta\|_2 \leq \|\Phi\beta\|_2 \leq (1+t)\sqrt{\frac{n}{m}}\|\beta\|_2 \quad (20)$$

The proof of Theorem 6 follows from the lemmas and from the proposition below. The proof for the following proposition is provided in the Supplementary Material.

Proposition 9. *We have that:*

$$\left| \|\hat{\beta}\|_2 - \|\Phi\beta\|_2 \right| \leq \frac{1}{\sqrt{n}} \sqrt{\|\hat{\Sigma}^\dagger\|_2} \|\epsilon\|_2. \quad (21)$$

Proof of Theorem 6. From Proposition 9 we have $\|\hat{\beta}\|_2 \leq \|\Phi\beta\|_2 + \frac{\|\epsilon\|_2}{\sqrt{n}} \sqrt{\lambda_{\max}(\hat{\Sigma}^\dagger)}$. Due to the fact that the noise is sub-Gaussian, a straightforward application of Theorem 3.1.1 from [41] implies that $\left| \frac{\|\epsilon\|_2}{\sqrt{n}} - \sigma^2 \right| \leq t$ with probability greater than $1 - 2 \exp(ct^2n)$. This together with Lemma 7 results in the desired upper bound for the second term. The first term can be bounded using Lemma 8, which yields the desired result. \square

We mention here that Lemma 4 could provide another possible route to prove similar results and (most likely) tighter bounds. Nonetheless, here, we choose to use Proposition 9 for two reasons: 1) it can be easily combined with non-asymptotic results; 2) the same argument applied above can be extended for any other p -norms. We also point out that an analogous procedure could be used to provide a lower bound on $\|\hat{\beta}\|_2$.

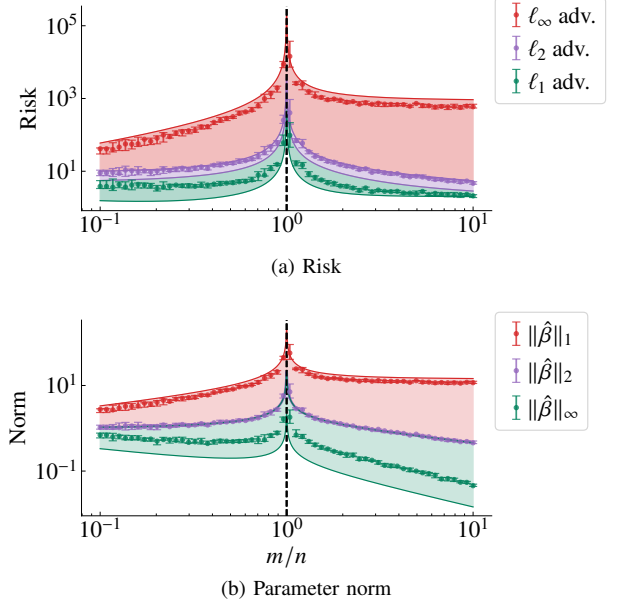


Fig. 3: Adversarial ℓ_p risk, isotropic features. The error bars give the median and the 0.25 and 0.75 quantiles obtained from numerical experiments (10 realizations) with a fixed training dataset of size $n = 100$ and for adversarial disturbances of magnitude $\delta = 2$. The shaded region in blue give the upper and lower bounds for $p = 2$. The bounds obtained from norm inequalities (22) for $p, q \in \{1, \infty\}$ are given in red and green. The results are for $r^2 = 1$, $\sigma^2 = 1$.

E. ℓ_p adversaries

We now turn to the study of ℓ_p adversarial attacks when $p \neq 2$. As in Eq. (16), let q be the complement of p . The following well-known relationship between vector norms will be useful in our developments.

Lemma 10 (Relationship between vector p -norms). *Let p and q be values in the range $[1, \infty]$ and $\hat{\beta} \in \mathbb{R}^m$. Assume that $q > p$, then:*

$$\|\hat{\beta}\|_q \leq \|\hat{\beta}\|_p \leq m^{1/p-1/q} \|\hat{\beta}\|_q. \quad (22)$$

The leftmost inequality follows from an application of Minkowski's inequality and the rightmost from an application of Hölder's inequality.

The asymptotic results from Lemma 5 to compute R and L_2 can now be used in conjunction with the above inequalities to find the upper and lower bounds on the adversarial risk. Hence, for any $1 \leq p < 2$, the upper bound is the same as the upper bound obtained for ℓ_2 attacks. However, there is a new multiplicative term in the lower bound. For instance, the ℓ_1 adversarial risk is bounded by

$$R(\hat{\beta}) + \frac{\delta^2}{m} \|\hat{\beta}\|_2^2 \leq R_1^{\text{adv}}(\hat{\beta}) \leq \left(\sqrt{R(\hat{\beta})} + \delta \|\hat{\beta}\|_2 \right)^2. \quad (23)$$

On the other hand, for ℓ_p adversarial attacks with $p > 2$, we obtain an asymptotic upper bound that grows with $m^{1-\frac{2}{p}}$. As an example, for ℓ_∞ attacks,

$$R(\hat{\beta}) + \delta^2 \|\hat{\beta}\|_2^2 \leq R_\infty^{\text{adv}}(\hat{\beta}) \leq \left(\sqrt{R(\hat{\beta})} + \delta \sqrt{m} \|\hat{\beta}\|_2 \right)^2. \quad (24)$$

In Figure 3(a) we illustrate the bounds obtained in this way. We note that the ℓ_∞ adversarial risk follows the upper bound closely. Moreover, Lemma 10 implies that

$$\|\hat{\beta}\|_2 \leq \|\hat{\beta}\|_1 \leq \sqrt{m}\|\hat{\beta}\|_2. \quad (25)$$

From Figure 3(b) we see that the ℓ_1 norm of the estimated parameter seemingly follows the upper bound closely. The adversarial risk also seems to follow the upper bound closely. Next, we provide some insight into this observation, by following the same steps used in the non-asymptotic analysis of the ℓ_2 parameter norm.

Lemma 8 show how $\|\Phi\beta\|_2$ concentrate around $\sqrt{\frac{n}{m}}\|\beta\|_2$. One might wonder whether similar concentration inequalities can be obtained also for the ℓ_1 norm. In Figure 4 we illustrate the experiments for both $\|\Phi\beta\|_1$ and $\|\Phi\beta\|_2$. The first plot just illustrate the results known from the ℓ_2 norm (i.e. Lemma 8) the second plot seem to suggest that the ℓ_1 norm of the projection concentrates around $c\sqrt{n}\|\beta\|_2$. From the experiments, we also estimate that $c \approx 0.8$. We state this result as a conjecture.

Conjecture 11. *Let Φ be a projection from \mathbb{R}^m onto a random n -dimensional subspace uniformly sampled from $G(m, n)$. Let $\beta \in \mathbb{R}$. Then, there is a constant c such that,*

$$\|\Phi\beta\|_1 - c\sqrt{n}\|\beta\|_2 < t$$

with probability higher then $p(t)$.

We leave the proof of this conjecture for future work. Here, we limit ourselves to point out that this conjecture does have important consequences for the study of overparameterized models: the idea that overparameterization yield smoother models is at the heart of the explanation of their good performance. The conjecture shows that, while this might be the case for the ℓ_2 norm, it might not be the case for the ℓ_1 norm. Indeed, the conjecture implies that with high probability

$$\left| \frac{\|\Phi\beta\|_1}{\|\Phi\beta\|_2} - c\sqrt{m}\|\beta\|_2 \right| < t. \quad (26)$$

Now, using exactly the same argument as in Lemma 9, we obtain

$$\|\Phi\beta\|_1 - \|\epsilon\|_2 \sqrt{\frac{m}{n}\|\hat{\Sigma}^\dagger\|_2} \leq \|\hat{\beta}\|_1 \leq \|\Phi\beta\|_1 + \|\epsilon\|_2 \sqrt{\frac{m}{n}\|\hat{\Sigma}^\dagger\|_2}$$

The conjecture implies that $\|\Phi\beta\|_1 = \Theta(\sqrt{n})\|\beta\|_2$, and Lemma 7 implies that the second term is $\Theta(\sqrt{n})\|\epsilon\|_2$. Hence, for a sufficiently large signal-to-noise ratio ($r > \sigma$) it follows from the conjecture that $\|\hat{\beta}\|_1 = \Theta(\sqrt{n})$. Since we obtained in the Theorem 6 that $\|\hat{\beta}\|_2 = \Theta(\sqrt{\frac{n}{m}})$, it follows that $\|\hat{\beta}\|_1 = \Theta(\sqrt{m})\|\hat{\beta}\|_2$, which is consistent with the results we are experimentally observing.

F. Scaling

The scaling of variables plays an important role in the analysis. Assume that a given $\hat{\beta}$ was estimated and the corresponding model prediction is $\hat{\beta}^\top x$. By simply redefining the input variable as $\tilde{x} = \frac{1}{\eta}x$ we could obtain an equivalent model $\tilde{\beta}^\top \tilde{x}$ that, for $\tilde{\beta} = \eta\hat{\beta}$, would yield exactly the same predictions.

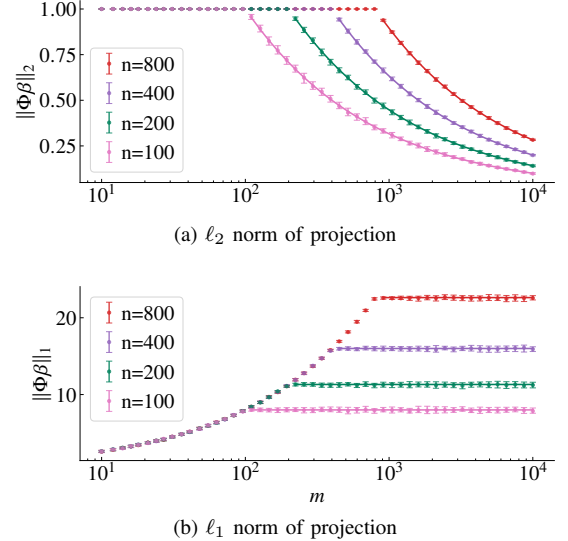


Fig. 4: Random projection and norms. Let Φ be a (uniform) random projection from \mathbb{R}^m into a subspace of dimension m . The full lines give the values predicted when $m < n$: $(m/n)^{-1/2}$ for the ℓ_2 norm; and, the constant rate $c\sqrt{n}$ for $c = 0.8$ for the ℓ_1 norm. The error bars give the median and interquartile range of 100 experiments.

Notice that while the standard risk R for this new, rescaled, model is exactly the same as the first, the norm of the estimated parameter $\|\tilde{\beta}\|_q$ is η times larger. The adversarial risk is not the same for the two models, as an inspection of Eq. (16) reveals. The difference is because the *relative* magnitude of the adversarial disturbance is larger in the second model (even though it is the same in absolute value).

Since we are interested in the impact that the number of parameters m has on adversarial robustness, we will let the scaling factor depend on this parameter, i.e. $\eta = \eta(m)$. The next proposition motivates two choices of scaling. The proof is provided in the Supplementary Material.

Proposition 12. *Let x be an isotropic random vector, $\mathbb{E}[\|x\|_2^2] = m$. Additionally, if x is a sub-Gaussian random vector, then $\mathbb{E}[\|x\|_\infty] = \Theta(\sqrt{\log(m)})$.*

Hence, either $\eta(m) = \sqrt{m}$ or $\eta(m) = \sqrt{\log m}$ are quite natural choices of the scaling factor. They render, respectively, the expected ℓ_2 and ℓ_∞ norms of the input vector constant as the number of features m varies.

Assume that the inputs are redefined as $\tilde{x}_i = \frac{1}{\eta(m)}x_i$. A quick inspection of Eq. (12) reveals that the estimated parameter is $\tilde{\beta} = \eta(m)\hat{\beta}$. The risk $R(\tilde{\beta})$ does not change by the transformation, but the expected squared norm of the parameter does, $\|\tilde{\beta}\|_2^2 = (\eta(m))^2\|\beta\|_2^2$. Hence, when $\eta(m) = \sqrt{\log m}$, it follows from Eq. (19) that

$$\|\tilde{\beta}\|_2^2 \approx \log m \left(r^2 \frac{1}{m/n} + \sigma^2 \frac{1}{m/n - 1} \right). \quad (27)$$

Here, the logarithmic term changes slowly compared to the linear term in the denominator. Hence, the result is similar to

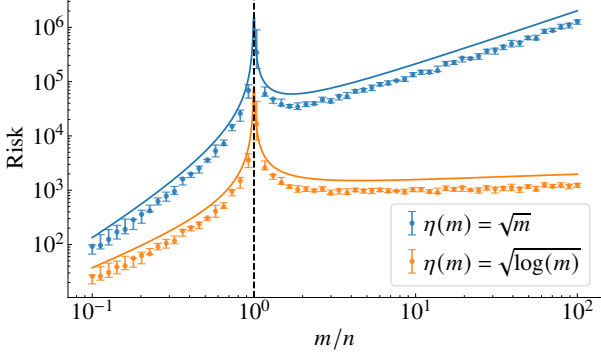


Fig. 5: **Adversarial ℓ_∞ risk, isotropic features.** The asymptotic upper bound is indicated by the full trace. The error bars give the median and the 0.25 and 0.75 quantiles obtained from numerical experiments (10 realizations). The analysis is performed for a fixed training dataset of size $n = 100$ and for adversarial disturbances of magnitude $\delta = 0.1$. The results are for $r^2 = 1$, $\sigma^2 = 1$. We show the results for two different scalings: $\eta(m) = \sqrt{m}$ and $\eta(m) = \sqrt{\log(m)}$.

what was obtained without any scaling. On the other hand, the square root scaling $\eta(m) = \sqrt{m}$ yields:

$$\|\tilde{\beta}\|_2^2 \approx r^2 n + \sigma^2 \frac{1}{1/n - 1/m}. \quad (28)$$

Here, the parameter norm does not go to zero. Instead, it approaches a constant as $m \rightarrow \infty$. The behavior is illustrated in Figure S.1 in the Supplementary material. One interesting consequence of Eq. (28) is that $\|\tilde{\beta}\|_2$ grows with the number of training datapoints. Hence, *the ℓ_2 adversarial performance degrades as we add more training data points*.

The situation is even more pathological in the case of ℓ_∞ adversarial attacks. In Figure 5, we show the ℓ_∞ adversarial risk as a function of m when the input is scaled by $\eta(m) = \sqrt{m}$ and $\eta(m) = \sqrt{\log(m)}$. We also provide the upper bound obtained from Lemma 5 and inequality (24). The behavior of ℓ_∞ adversarial attacks is governed by $\|\tilde{\beta}\|_1$ (see Eq. (10)) and we have $\|\tilde{\beta}\|_1 = \Theta(\sqrt{m})\|\tilde{\beta}\|_2$ (recall Section IV-E). Hence, (28) and (27) yield, respectively, $\|\tilde{\beta}\|_1 = \Theta(\sqrt{m})$ and $\|\tilde{\beta}\|_1 = \Theta(\sqrt{\log m})$, which explain the behavior we observe in the figure.

G. Latent space model

For the model studied in the previous section it is in general possible to achieve models with smaller test error in the underparameterized than in the overparameterized region. Thus, it could be argued that the lack of ℓ_∞ adversarial robustness in the overparameterized region should not be a problem in practice. Let us now illustrate a different data generation procedure for which we have better performance in the overparameterized regime and, as we add more features, the performance is continuously improved. It is still, however, possible to observe that the ℓ_∞ adversarial robustness degrades indefinitely with the number of features (recall Figure 1).

We consider a data model where the features x are noisy observations of a lower-dimensional subspace of dimension d .

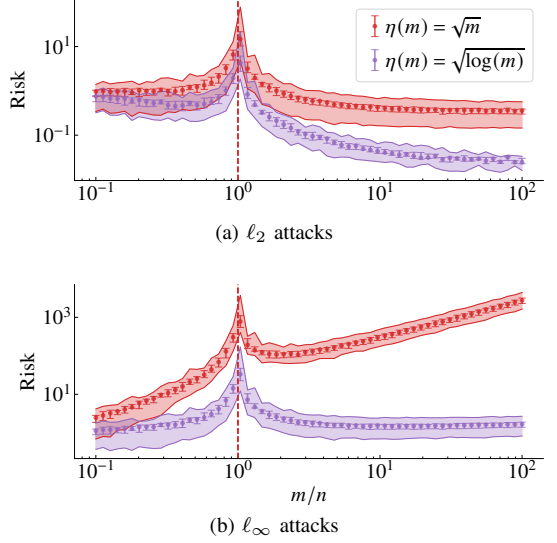


Fig. 6: **Adversarial risk for a latent model.** The median and interquartile range of the adversarial risk is obtained from numerical experiments (10 realizations) and indicated by error bars. Unlike the other plots, here the shaded region indicates the upper and lower bounds obtained empirically from Eq. (10). Where the empirical risk in the test and the parameter norm are obtained from the experiments. The analysis is performed for adversarial disturbances of magnitude $\delta = 0.1$ and for a training dataset with size $n = 200$. The results are for $\sigma_\xi^2 = 0.1$ and for a latent space with constant dimension $d = 20$. We show the results for two different scalings: $\eta(m) = \sqrt{m}$ and $\eta(m) = \sqrt{\log(m)}$.

A vector in this *latent space* is represented by $z \in \mathbb{R}^d$. This vector is indirectly observed via the features $x \in \mathbb{R}^m$ according to

$$x = Wz + u, \quad (29)$$

where W is a $m \times d$ matrix, for $m \leq d$. We assume that the responses are described by a linear model in this latent space

$$y = \theta^\top z + \xi, \quad (30)$$

where $\xi \in \mathbb{R}$ and $u \in \mathbb{R}^m$ are mutually independent noise variables. Moreover, $\xi \sim \mathcal{N}(0, \sigma_\xi^2)$ and $u \sim \mathcal{N}(0, I_m)$. We consider the features in the latent space to be isotropic and normal $z_i = \mathcal{N}(0, I_d)$. To facilitate the analysis, we choose W such that its columns are orthogonal, $W^\top W = \frac{m}{d} I_d$, where the factor $\frac{m}{d}$ is introduced to guarantee that the signal-to-noise ratio of the feature vector x (i.e. $\frac{\|Wz\|_2^2}{\|u\|_2^2}$) is kept constant.

This model is related to the other setups we have presented so far. The weak feature example (Section IV-A) is a special case of this model class with $\theta = 1$, $\sigma_\xi = 0$, and $W = 1$. Moreover, this latent model can actually be written as in Eq. (11), as we show in the Supplementary Material Section D.

Assume a training dataset $\{(x_i, y_i)\}_{i=1}^n$ generated using the above procedure. To this data we fit a linear model $\hat{\beta}x_i$ using the minimum-norm solution. Most of the arguments we presented for the isotropic case can be reused here. Asymptotics from Hastie *et al.* [7] are available in the Supplementary

Material. From our non-asymptotic analysis in the isotropic case we obtained $\|\hat{\beta}\|_2 = \mathcal{O}\left(\frac{1}{\sqrt{m/n}}\right)$, the same rate is obtained here. See Supplementary Material Section D.

If again, we allow the input to be scaled, i.e. $\tilde{x}_i = \frac{1}{\eta(m)}x_i$, a similar analysis shows that the factors $\eta(m) = \sqrt{m}$ and $\eta(m) = \sqrt{\log(m)}$ would correspond to keeping $\mathbb{E}_x[\|x\|_2]$ and $\mathbb{E}_x[\|x\|_\infty]$ constant, respectively. In Figure 6 we illustrate the results for the two scalings and a fixed latent dimension $d = 20$. We observe that the adversarial ℓ_2 risk, for both input scalings, continuously decrease in the overparameterized region and achieve better results there than in the underparameterized region. The adversarial ℓ_∞ risk, on the other hand, presents quite a different behavior depending on the scaling. For $\eta(m) = \sqrt{m}$ it displays a linear growth with the number of parameters in the overparameterized region, while it remains basically constant in the case $\eta(m) = \sqrt{\log(m)}$. Figure 1 is an illustration of this same setting where we also include the standard risk in the same plot (scaling $\eta(m) = \sqrt{m}$). Additional results are presented in Supplementary Material Section D.

V. ADVERSARIAL TRAINING AND REGULARIZATION

Empirical risk minimization (ERM) has been tremendously successful in finding predictors with good performance. In the last section, the model was trained to minimize the empirical risk $\hat{R}(\beta)$ but evaluated according to an adversarial criteria. One natural idea to obtain models that are more robust to adversarial attacks is to instead minimize the empirical adversarial risk,

$$\hat{R}_p^{\text{adv}}(\hat{\beta}) = \frac{1}{n} \sum_{i=1}^n \max_{\|\Delta x_i\|_p \leq \delta} (y_i - (x_i + \Delta x_i)^\top \hat{\beta})^2. \quad (31)$$

This method is commonly called adversarial training [8].

In this section, we use Lemma 2 to develop a convex formulation of adversarial training for linear regression problems. With this tool in hand, we explore the effect of adversarial training on how the model robustness changes the number of features. We also compare it to ridge regression,

$$\hat{R}_{\text{ridge}}(\hat{\beta}) = \frac{1}{n} \sum_{i=1}^n (y_i - x_i^\top \hat{\beta})^2 + \delta \|\hat{\beta}\|_2^2, \quad (32)$$

and lasso,

$$\hat{R}_{\text{lasso}}(\hat{\beta}) = \frac{1}{n} \sum_{i=1}^n (y_i - x_i^\top \hat{\beta})^2 + \delta \|\hat{\beta}\|_1. \quad (33)$$

A. Adversarial training using convex programming

Using Lemma 2 it is easy to show the convexity of the adversarial risk (defined in Eq. (2)).

Proposition 13. For $p \in [1, \infty]$, $R_p^{\text{adv}}(\hat{\beta})$ is convex in β .

Proof. Let $\gamma \in [0, 1]$, for $q \in [1, \infty]$, $\|\hat{\beta}\|_q$ is a norm and from the triangular inequality, we have that:

$$\|\gamma\hat{\beta}_1 + (1-\gamma)\hat{\beta}_1\|_q \leq \gamma\|\hat{\beta}_1\|_q + (1-\gamma)\|\hat{\beta}_2\|_q \quad (34)$$

Moreover,

$$|y_0 - x_0^\top (\gamma\hat{\beta}_1 + (1-\gamma)\hat{\beta}_1)| \leq \gamma|y_0 - x_0^\top \hat{\beta}_1| + (1-\gamma)|y_0 - x_0^\top \hat{\beta}_2|.$$

Hence, $h(\hat{\beta}) = |y_0 - x_0^\top \hat{\beta}| + \|\hat{\beta}\|_q$ is convex and, also, $h(\hat{\beta}) \geq 0$ for all $\hat{\beta}$. Now, since $g(x) = x^2$ is convex and non-decreasing for $x \geq 0$, the composition $g \circ h$ is convex – See Boyd *et al.* [42, Section 3.2.4]; moreover, the expected value of a convex function is also convex [42, Section 3.2.1] and it follows that the right-hand side of Eq. (5) is convex. \square

The results obtained for the adversarial risk are also valid for the empirical adversarial risk. Hence, it follows from Lemma 2 that:

$$\hat{R}_p^{\text{adv}}(\hat{\beta}) = \frac{1}{n} \sum_{i=1}^n \left(|y_i - x_i^\top \hat{\beta}| + \delta \|\hat{\beta}\|_q \right)^2, \quad (35)$$

and that it is convex. The above expression can be entered in a standard convex modeling language to obtain the adversarial training solution. In the numerical examples that follows we use CVXPY [43] to train the model.

B. Overparameterized models: Latent space feature model

In this example, we consider artificially generated data from the latent space feature model described in Section IV. The same experiment for the isotropic feature model is provided in the Supplementary Material Section E. In Section IV, we saw the unfortunate effect that if the input variables scale with $\eta(m) = \sqrt{m}$ (which corresponds to keeping $\mathbb{E}[\|x\|_2]$ constant as we vary the number of features m) we observe that $\|\hat{\beta}\|_1$ grows indefinitely with m when $\hat{\beta}$ was estimated using the minimum-norm solution. We also showed how this makes the ℓ_∞ adversarial risk grow indefinitely with the number of features (i.e., Fig. 1).

Let us now investigate if the same effect can be observed for models trained with ridge regression, lasso and adversarial training. In Fig. 7 we show the norm $\|\hat{\beta}\|_1$ in these cases. Ridge regression displays the parameter norm growing with $\mathcal{O}(m)$ regardless of how large the regularization parameter δ is. We notice that ℓ_2 adversarial training has a similar behavior for δ smaller than a certain threshold, in these cases it displays curves similar to ridge regression that grow with $\mathcal{O}(m)$. However, for sufficiently large values of the regularization parameter, the parameter norm of the solution is zero for all values of m .

For lasso, we see that the parameter norm goes to zero for overparameterized models with sufficiently large m . Looking at lasso as a bi-objective optimization problem helps interpreting this behavior: as the number of features m increases, the scaling affects the two objectives differently and the objective of keeping $\|\hat{\beta}\|_1$ starts to be prioritized over the objective of keeping the square training error low the more m is increased. Interestingly, the ℓ_∞ adversarial training seems to behave in a very similar way.

In Fig. 8 we provide the adversarial test error for models trained with ridge regression, lasso and adversarial training, respectively. As expected by our analysis of $\|\hat{\beta}\|_1$, lasso and ℓ_∞ adversarial training yield solutions that do not deteriorate indefinitely. We believe this observation adds to our discussion about the role of the scaling. It highlights the fact that, even in the case of a mismatch between disturbance and how the input scales with the number of variables (i.e., $\mathbb{E}_x[\|x\|_2^2]$ constant while we evaluate it under an ℓ_∞ adversary) it is still possible

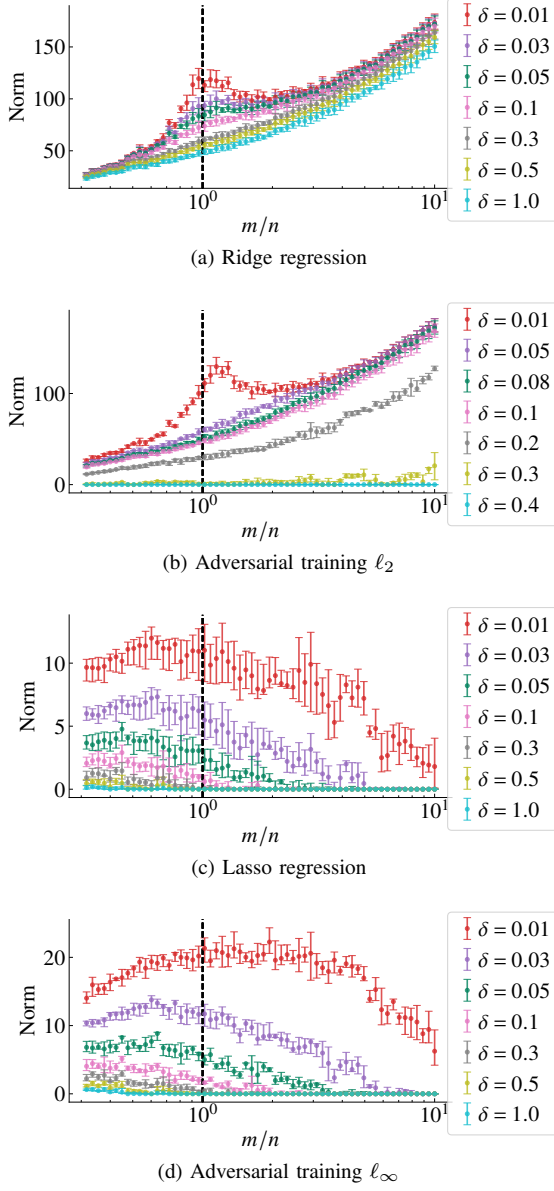


Fig. 7: **Parameter norm** $\|\hat{\beta}\|_1$. The input variables are scaled with $\eta(m) = \sqrt{m}$. The error bars give the median and the 0.25 and 0.75 quantiles obtained from numerical experiments (6 realizations) for a fixed training dataset of size $n = 100$. We repeat the experiment for different amounts of regularization. The regularization parameter δ defined in Eq. (31) for the adversarial training and in Eq. (32) and (33) for ridge regression and lasso. It is indicated in the plot by the different colors.

to avoid brittleness by considering a type of regularization that acts under the right norm.

VI. DISCUSSION AND CONCLUSION

A question that naturally comes to mind is if parts of this analysis can be generalized to nonlinear settings. Let us define the adversarial risk associated with a given function f by:

$$R_p^{\text{adv}}(f) = \mathbb{E}_{x_0, y_0} \left[\max_{\|\Delta x_0\|_p \leq \delta} (y_0 - f(x_0 + \Delta x_0))^2 \right]. \quad (36)$$

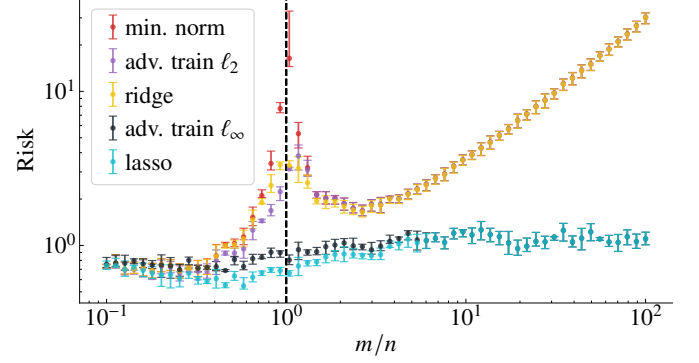


Fig. 8: **Adversarial ℓ_∞ risk.** On the y -axis we show the ℓ_∞ adversarial risk for models obtained by different training methods. On the x -axis we have the ratio between the number of features m and the number of training datapoints n . The error bars give the median and the 0.25 and 0.75 quantiles obtained from numerical experiments (6 realizations). We use $\delta = 0.01$ both during inference (to compute the adversarial risk) and during the adversarial training, as in Eq. (31). We also use $\delta = 0.01$ for lasso and ridge regression, see Eq. (32) and (33).

It is possible to obtain an upper bound similar to the one in Eq. (10). Let $L(f)$ be the Lipschitz constant of f , i.e. $|f(x_1) - f(x_2)| \leq L(f)\|x_1 - x_2\|$ for all x_1, x_2 . An analysis equivalent to the one used in the proof of Lemma 2 yields

$$R_p^{\text{adv}}(f) \leq \mathbb{E}_{x_0, y_0} \left[(|y_0 - f(x_0)| + \delta L(f))^2 \right]. \quad (37)$$

In this case, equality does not necessarily hold. Proposition 3 was used in the proof for the linear case, but there is not an obvious equivalent in the nonlinear case. Hence, instead of the approximation (8) we would only have $R_p^{\text{adv}}(f) \lesssim R(f) + \delta^2 L(f)^2$. Indeed, the idea of using the Lipschitz constant as a proxy for robustness is quite standard and a common procedure to obtain robust models is to jointly optimize the risk $R(f)$ and the Lipschitz constant $L(f)$, see e.g. [44]. However, studying the linear case still clarifies facts that are not obvious.

Indeed, we show in this paper that different definitions of the metrics used in the input space might result in completely different assessments of the robustness. For instance, we provided examples of models that are robust to ℓ_2 attacks, but can be made completely vulnerable to ℓ_∞ as we grow the number of features. While one could think of it as an aspect of the curse of dimensionality, we would like to stress that it does not reveal the full story, there are more aspects to be considered. The most pathological results are obtained in a mismatched setup, where we keep $\mathbb{E}_x [\|x\|_2^2]$ but apply an adversarial attack constrained by the ℓ_∞ norm: $\|\Delta x\|_\infty \leq \delta$. In this case, we have shown that the adversarial risk can be made arbitrarily large (i.e., the model is arbitrarily vulnerable to an adversary) as the number of features grows.

The idea that brittleness to adversarial examples is reproducible in linear models is highly influential, the mismatched setup resulting in brittleness is something that usually appears hidden in the argument but is present in many examples found

in the literature. In Section IV-A we show one example inspired by [13]. We cite Goodfellow *et al.* [5, Section 3] as another example of a highly influential work where an ℓ_∞ attack is considered while implicitly assuming the input ℓ_2 -norm is kept constant.

We also provided a convex optimization formulation for adversarial training and showed that there are similarities for the high-dimensional setup between ℓ_∞ adversarial training and lasso, and between ℓ_2 adversarial training and ridge regression. We intend to further explore the similarities and differences between these methods in future work. We also intend to further evaluate the effectiveness of adversarial training as a robust regression method.

ACKNOWLEDGEMENT

The authors would like to thank Dave Zachariah for very fruitful discussions throughout the work with this research. This research was financially supported by the project *Deep probabilistic regression – new models and learning algorithms* (contract number: 2021-04301), funded by the Swedish Research Council and by *Kjell och Märta Beijer Foundation*.

REFERENCES

- [1] M. Belkin, D. Hsu, S. Ma, and S. Mandal, “Reconciling modern machine-learning practice and the classical bias–variance trade-off,” *Proceedings of the National Academy of Sciences*, vol. 116, no. 32, pp. 15 849–15 854, 2019.
- [2] C. Zhang, S. Bengio, M. Hardt, B. Recht, and O. Vinyals, “Understanding deep learning requires rethinking generalization,” in *Proceedings of the 5th International Conference on Learning Representations (ICLR)*, 2017.
- [3] S. Bubeck and M. Sellke, “A Universal Law of Robustness via Isoperimetry,” *Advances in Neural Information Processing Systems*, 2021.
- [4] J. Bruna, C. Szegedy, I. Sutskever, I. Goodfellow, W. Zaremba, R. Fergus, and D. Erhan, “Intriguing properties of neural networks,” in *Proceedings of the 2nd International Conference on Learning Representations (ICLR)*, 2014.
- [5] I. J. Goodfellow, J. Shlens, and C. Szegedy, “Explaining and Harnessing Adversarial Examples,” in *Proceedings of the 3rd International Conference on Learning Representations (ICLR)*, 2015.
- [6] P. L. Bartlett, P. M. Long, G. Lugosi, and A. Tsigler, “Benign overfitting in linear regression,” *Proceedings of the National Academy of Sciences*, vol. 117, no. 48, pp. 30 063–30 070, 2020.
- [7] T. Hastie, A. Montanari, S. Rosset, and R. J. Tibshirani, “Surprises in High-Dimensional Ridgeless Least Squares Interpolation,” *arXiv:1903.08560*, 2019.
- [8] A. Madry, A. Makelov, L. Schmidt, D. Tsipras, and A. Vladu, “Towards Deep Learning Models Resistant to Adversarial Attacks,” *Proceedings of the International Conference for Learning Representations (ICLR)*, 2018.
- [9] R. Tibshirani, “Regression shrinkage and selection via the LASSO,” *Journal of the Royal Statistical Society. Series B (Methodological)*, pp. 267–288, 1996.
- [10] N. Dalvi, P. Domingos, Mausam, S. Sanghavi, and D. Verma, “Adversarial classification,” in *Proceedings of the Tenth ACM SIGKDD International Conference on Knowledge Discovery and Data Mining*, 2004.
- [11] A. Globerson and S. Roweis, “Nightmare at test time: Robust learning by feature deletion,” in *Proceedings of the 23rd International Conference on Machine Learning (ICML)*, 2006, pp. 353–360.
- [12] B. Biggio and F. Roli, “Wild patterns: Ten years after the rise of adversarial machine learning,” *Pattern Recognition*, vol. 84, pp. 317–331, 2018.
- [13] D. Tsipras, S. Santurkar, L. Engstrom, A. Turner, and A. Ma, “Robustness May Be At Odds with Accuracy,” *Proceedings of the International Conference for Learning Representations (ICLR)*, p. 23, 2019.
- [14] A. Ilyas, S. Santurkar, D. Tsipras, L. Engstrom, B. Tran, and A. Madry, “Adversarial Examples Are Not Bugs, They Are Features,” *Advances in Neural Information Processing Systems*, vol. 32, 2019.
- [15] J. Gilmer, L. Metz, F. Faghri, S. S. Schoenholz, M. Raghu, M. Wattenberg, and I. Goodfellow, “Adversarial Spheres,” *arXiv:1801.02774*, 2018.
- [16] D. Yin, R. Kannan, and P. Bartlett, “Rademacher Complexity for Adversarially Robust Generalization,” in *Proceedings of the 36th International Conference on Machine Learning*, PMLR, 2019, pp. 7085–7094.
- [17] S. Bubeck, Y. Li, and D. Nagaraj, “A law of robustness for two-layers neural networks,” *134 of Proceedings of Machine Learning Research, Conference on Learning Theory (COLT)*, vol. 134, pp. 804–820, 2021.
- [18] A. Daniely and H. Shacham, “Most ReLU Networks Suffer from ℓ_2 Adversarial Perturbations,” in *Advances in Neural Information Processing Systems*, vol. 33, 2020, pp. 6629–6636.
- [19] P. L. Bartlett, S. Bubeck, and Y. Cherapanamjeri, “Adversarial Examples in Multi-Layer Random ReLU Networks,” *Neural Information Processing Systems (NeurIPS)*, 2021.
- [20] P. Nakkiran, G. Kaplun, Y. Bansal, T. Yang, B. Barak, and I. Sutskever, “Deep Double Descent: Where Bigger Models and More Data Hurt,” in *Proceedings of the 8th International Conference on Learning Representations (ICLR)*, 2020.
- [21] M. Geiger, S. Spigler, S. d’Ascoli, L. Sagun, M. Baity-Jesi, G. Biroli, and M. Wyart, “Jamming transition as a paradigm to understand the loss landscape of deep neural networks,” *Physical Review E*, vol. 100, no. 1, p. 012 115, 2019.
- [22] M. Geiger, A. Jacot, S. Spigler, F. Gabriel, L. Sagun, S. d’Ascoli, G. Biroli, C. Hongler, and M. Wyart, “Scaling description of generalization with number of parameters in deep learning,” *Journal of Statistical Mechanics: Theory and Experiment*, vol. 2020, no. 2, p. 023 401, 2020.
- [23] A. H. Ribeiro, J. N. Hendriks, A. G. Wills, and T. B. Schön, “Beyond Occam’s Razor in System Identification: Double-Descent when Modeling Dynamics,” in *Proceedings of the 19th IFAC Symposium on System*

Identification (SYSID) - IFAC-PapersOnLine, vol. 54, Elsevier, 2021, pp. 97–102.

[24] Z. Deng, A. Kammoun, and C. Thrampoulidis, “A Model of Double Descent for High-Dimensional Logistic Regression,” in *ICASSP 2020 - 2020 IEEE International Conference on Acoustics, Speech and Signal Processing (ICASSP)*, 2020, pp. 4267–4271.

[25] V. Muthukumar, K. Vodrahalli, V. Subramanian, and A. Sahai, “Harmless Interpolation of Noisy Data in Regression,” *IEEE Journal on Selected Areas in Information Theory*, vol. 1, no. 1, pp. 67–83, 2020.

[26] A. D’Amour, K. Heller, D. Moldovan, *et al.*, “Underspecification Presents Challenges for Credibility in Modern Machine Learning,” *arXiv:2011.03395*, 2020.

[27] S. Mei and A. Montanari, “The Generalization Error of Random Features Regression: Precise Asymptotics and the Double Descent Curve,” *Communications on Pure and Applied Mathematics*, vol. 75, no. 4, pp. 667–766, 2022.

[28] J. Pennington and P. Worah, “Nonlinear random matrix theory for deep learning,” in *Advances in Neural Information Processing Systems*, 2017, pp. 2637–2646.

[29] J. Pennington, S. S. Schoenholz, and S. Ganguli, “The Emergence of Spectral Universality in Deep Networks,” *21st International Conference on Artificial Intelligence and Statistics (AISTATS)*, 2018.

[30] L. Pastur, “On Random Matrices Arising in Deep Neural Networks. Gaussian Case,” *arXiv:2001.06188*, 2020.

[31] M. Belkin, D. Hsu, and J. Xu, “Two Models of Double Descent for Weak Features,” *SIAM Journal on Mathematics of Data Science*, vol. 2, no. 4, pp. 1167–1180, 2020.

[32] M. S. Advani, A. M. Saxe, and H. Sompolinsky, “High-dimensional dynamics of generalization error in neural networks,” *Neural Networks*, vol. 132, pp. 428–446, 2020.

[33] B. Adlam and J. Pennington, “The Neural Tangent Kernel in High Dimensions: Triple Descent and a Multi-Scale Theory of Generalization,” *Proceedings of the 37 th International Conference on Machine Learning, PMLR 119*, 2020.

[34] A. N. Bhagoji, D. Cullina, and P. Mittal, “Lower Bounds on Adversarial Robustness from Optimal Transport,” *Advances in Neural Information Processing Systems*, vol. 32, 2019.

[35] D. Diocno, S. Mahloujifar, and M. Mahmoody, “Adversarial risk and robustness: General definitions and implications for the uniform distribution,” in *Advances in Neural Information Processing Systems*, vol. 31, 2018.

[36] H. Taheri, R. Pedarsani, and C. Thrampoulidis, “Asymptotic Behavior of Adversarial Training in Binary Classification,” *arXiv:2010.13275*, 2021.

[37] A. Javanmard, M. Soltanolkotabi, and H. Hassani, “Precise tradeoffs in adversarial training for linear regression,” in *Proceedings of 33rd Conference on Learning Theory*, vol. 125, PMLR, 2020, pp. 2034–2078.

[38] A. Javanmard and M. Soltanolkotabi, “Precise Statistical Analysis of Classification Accuracies for Adversarial Training,” *arXiv:2010.11213*, 2020.

[39] H. Hassani and A. Javanmard, “The curse of overparametrization in adversarial training: Precise analysis of robust generalization for random features regression,” *arXiv:2201.05149*, 2022.

[40] Y. Min, L. Chen, and A. Karbasi, “The Curious Case of Adversarially Robust Models: More Data Can Help, Double Descent, or Hurt Generalization,” *roceedings of the Thirty-Seventh Conference on Uncertainty in Artificial Intelligence*, vol. 161, pp. 129–139, 2021.

[41] R. Vershynin, *High-Dimensional Probability*, ser. Cambridge Series in Statistical and Probabilistic Mathematics. Cambridge University Press, 2018.

[42] S. P. Boyd and L. Vandenberghe, *Convex Optimization*. Cambridge University Press, 2004.

[43] S. Diamond and S. Boyd, “CVXPY: A Python-embedded modeling language for convex optimization,” *Journal of Machine Learning Research*, vol. 17, no. 83, pp. 1–5, 2016.

[44] M. Fazlyab, A. Robey, H. Hassani, M. Morari, and G. J. Pappas, “Efficient and Accurate Estimation of Lipschitz Constants for Deep Neural Networks,” *Advances in Neural Information Processing Systems (NeurIPS)*, 2019.

Supplementary Material

Overparameterized Linear Regression under Adversarial Attacks

APPENDIX A PROOFS

A. Inequalities (10) and (16)

The two inequalities (10) and (16) follow from (7). The first can be derived by a direct application of Jensen's inequality that yields $0 \leq \mathbb{E}_{x_0, y_0} [|e_0|] \leq \sqrt{R(\hat{\beta})}$. The second inequality follows from a direct application of the Cauchy-Schwartz inequality: $0 \leq \mathbb{E}_{y, x_0, y_0} [\|\hat{\beta}\|_q |e_0|] \leq \sqrt{L_q R}$.

B. Proof of Lemma 4

The following decomposition is implicitly used through the paper. In Eq. (14) below, the risk is decomposed into: a term that can be understood as the model bias, another term that corresponds to the model variance, and the unavoidable risk σ^2 .

Proof. Proof for $\|\hat{\beta}\|_2$: From Eq. (11) and Eq. (12) it follows that:

$$\hat{\beta} = \underbrace{(X^\top X)^\dagger X^\top X \beta}_{\Phi} + \underbrace{(X^\top X)^\dagger X^\top \epsilon}_{\frac{1}{n} \hat{\Sigma}^\dagger}. \quad (\text{S.1})$$

Hence, since $\hat{\Sigma}$ is symmetric:

$$\hat{\beta}^\top \hat{\beta} = \beta^\top \Phi^\top \Phi \beta + \frac{1}{n} \beta^\top \Phi^\top \hat{\Sigma}^\dagger X^\top \epsilon + \frac{1}{n^2} \epsilon^\top X \hat{\Sigma}^\dagger \hat{\Sigma}^\dagger X^\top \epsilon, \quad (\text{S.2})$$

where the first term is equal to $\beta^\top \Phi \beta$ since, Φ is an *orthogonal projector* i.e., $\Phi^\top = \Phi$ and $\Phi \Phi = \Phi$. Moreover, the middle term has zero expectation.

Now, since the second term is a scalar, it is equal to its trace. Using the fact that the trace is invariant over cyclic permutations,

$$\epsilon^\top X \hat{\Sigma}^\dagger \hat{\Sigma}^\dagger X^\top \epsilon = \text{tr} \left\{ \hat{\Sigma}^\dagger X^\top \epsilon \epsilon^\top X \hat{\Sigma}^\dagger \right\}. \quad (\text{S.3})$$

From the assumption that the noise samples are independent and have variance σ^2 , we have $\mathbb{E}_\epsilon [\epsilon \epsilon^\top] = \sigma^2 I$, where I is the identity matrix. Since we can swap the trace and the expectation operator we obtain

$$\mathbb{E}_\epsilon [\hat{\beta}^\top \hat{\beta}] = \beta^\top \Phi \beta + \frac{1}{n^2} \text{tr} \left\{ \hat{\Sigma}^\dagger X^\top \underbrace{\mathbb{E}_\epsilon [\epsilon \epsilon^\top]}_{\sigma^2 I} X \hat{\Sigma}^\dagger \right\}.$$

The results follow from the definition of $\hat{\Sigma}^\dagger$ and the following property of pseudo-inverse $\hat{\Sigma}^\dagger \hat{\Sigma} \hat{\Sigma}^\dagger = \hat{\Sigma}^\dagger$.

Proof for R : Now,

$$R(\hat{\beta}) = \mathbb{E}_{x_0, y_0} [(\beta^\top x_0 - y_0)^2] = (\beta - \hat{\beta})^\top \Sigma (\beta - \hat{\beta}) + \sigma^2. \quad (\text{S.4})$$

From (S.1) it follows that:

$$\beta - \hat{\beta} = \underbrace{(I - \Phi)}_{\Pi} \beta + \frac{1}{n} \hat{\Sigma}^\dagger X^\top \epsilon,$$

where Π is again an orthogonal projector, i.e., $\Pi^\top = \Pi$ and $\Pi \Pi = \Pi$. We can then compute a closed-form expression for $\mathbb{E}_\epsilon [R(\hat{\beta})]$ using the same procedure. □

C. Proof of Lemma 7

From the lemma statement: x_i are independently sampled sub-Gaussian vectors. Let X be a matrix containing the vectors x_i as its rows, i.e.,

$$X = \begin{bmatrix} \cdots & x_1 & \cdots \\ \vdots & \vdots & \vdots \\ \cdots & x_n & \cdots \end{bmatrix}.$$

Let $s_i(X)$ denote the i -th singular value of X . From Vershynin [41, Theorem 4.6.1] we have that there exist a constant C such that with probability larger than $1 - 2 \exp(-t^2)$,

$$\sqrt{n} - C(\sqrt{m} + t) \leq s_i(X) \leq \sqrt{n} + C(\sqrt{m} + t), \quad \forall i = 1, \dots, n \quad (\text{S.5})$$

Set $t = \sqrt{m}$ then, since $\lambda_i(\hat{\Sigma}) = \left(\frac{1}{\sqrt{n}} s_{(n-i)}(X)\right)^{-2}$ we obtain with probability greater than $1 - 2 \exp(-m)$ that

$$\frac{1}{(1 + C(\sqrt{\frac{m}{n}}))^2} \leq \lambda_i(\hat{\Sigma}) \leq \frac{1}{(1 - C(\sqrt{\frac{m}{n}}))^2}, \quad \forall i = 1, \dots, n. \quad (\text{S.6})$$

Finally, since $m > n$, we have that $1 - 2 \exp(-m) > 1 - 2 \exp(-n)$ and the result follows.

D. Proof of Lemma 9

From Eq. (13) and the triangular inequality:

$$\left\| \|\hat{\beta}\|_2 - \|\Phi\beta\|_2 \right\| \leq \frac{1}{\sqrt{n}} \left\| \frac{1}{\sqrt{n}} \hat{\Sigma}^\dagger X^\top \epsilon \right\|_2 \quad (\text{S.7})$$

In turn, we have that

$$\left\| \frac{1}{n} \hat{\Sigma}^\dagger X^\top \epsilon \right\|_2 \leq \left\| \frac{1}{\sqrt{n}} \hat{\Sigma}^\dagger X^\top \right\|_2 \|\epsilon\|_2.$$

Note that for a matrix $A \in \mathbb{R}^{m \times n}$ we use $\|A\|_2$ to denote the operator norm. We have $\|A\|_2 = \max_i \sqrt{\lambda_i(A^\top A)}$. Hence:

$$\left\| \frac{1}{n} \hat{\Sigma}^\dagger X^\top \right\|_2 = \max_i \sqrt{\lambda_i(\hat{\Sigma}^\dagger \hat{\Sigma} \hat{\Sigma}^\dagger)} = \sqrt{\|\hat{\Sigma}^\dagger\|_2},$$

where the second equality follows by making direct use of the property $\hat{\Sigma}^\dagger \hat{\Sigma} \hat{\Sigma}^\dagger = \hat{\Sigma}^\dagger$ and by using the fact that $\hat{\Sigma}^\dagger$ is positive semidefinite.

E. (Partial) Proof of Proposition 12

Here $x \in \mathbb{R}^m$. To compute the expected ℓ_2 -norm of x_i we use the fact that $\text{Cov}[x] = I_m$,

$$\mathbb{E}_x [\|x\|_2^2] = \mathbb{E}_x [\text{tr}\{xx^\top\}] = \text{tr}\{\mathbb{E}_x [xx^\top]\} = \text{tr}\{I_m\} = m. \quad (\text{S.8})$$

Let us proceed by analyzing the ℓ_∞ -norm. Let $t > 0$ be an arbitrary value to be chosen later. Via direct use of Jensen's inequality we obtain

$$\exp(t\mathbb{E}_x [\|x\|_\infty]) \leq \mathbb{E} [\exp(t\|x\|_\infty)] = \mathbb{E} \left[\max_j \exp(t|x^j|) \right] \leq \sum_{j=1}^m (\mathbb{E} [\exp(t|x^j|)]). \quad (\text{S.9})$$

Using the fact that x^j is sub-Gaussian (without loss of generality, we assume unitary proxy variance), we have $\mathbb{E} [\exp(t|x^j|)] \leq \exp(t^2/2)$. Therefore,

$$\exp(t\mathbb{E} [\|x\|_\infty]) \leq 2m \exp(t^2/2). \quad (\text{S.10})$$

Therefore,

$$\mathbb{E} [\|x\|_\infty] \leq \frac{\log(2m)}{t} + \frac{t}{2}. \quad (\text{S.11})$$

Here, we can choose $t = 2\sqrt{\log(2m)}$, which yields

$$\mathbb{E} [\|x\|_\infty] \leq \sqrt{2 \log(2m)}. \quad (\text{S.12})$$

We conclude that $\mathbb{E} [\|x\|_\infty] = \mathcal{O}(\sqrt{\log(m)})$. It is also possible to obtain $\mathbb{E} [\|x\|_\infty] = \Omega(\sqrt{\log(m)})$ using a similar argument to the one described in "Bounds on the Expectation of the Maximum of Samples from a Gaussian" by Gautam Kamath (www.gautamkamath.com/writings/gaussian_max.pdf [online accessed: 2021-10-11]). Hence, $\mathbb{E} [\|x\|_\infty] = \Theta(\sqrt{\log(m)})$. The result for is also provided in Vershynin [41, Exercises 2.5.10 and 2.5.11].

APPENDIX B

ISOTROPIC FEATURE MODEL

The asymptotic behavior of R and L_2 for isotropic features is described in Lemma 5. In Figure S.1(a), we illustrate the behavior of the risk for different values of r^2 . Again, as in the main text, we refer to the “null risk” as the quantity $r^2 + \sigma^2$ that correspond to the risk of the null estimator $\hat{\beta} = 0$. In the underparameterized region, the prediction risk is smaller than the null risk iff $\frac{m}{n} < \frac{r^2}{\sigma^2 + r^2}$. In the overparameterized region, when $r^2 > \sigma^2$, as in the situation studied in the main text, the prediction risk has a local minima at $\gamma = \frac{r}{r + \sigma}$. Furthermore, it approaches the null risk from below as $\gamma \rightarrow \infty$. If $r^2 < \sigma^2$, the prediction risk decreases monotonically, approaching the null risk from above as $\gamma \rightarrow \infty$. As mentioned in the main text, the prediction risk does not change as the inputs are rescaled. However, the parameter norm does change. The parameter norm is shown for different scaling in Figure S.1(b). We discuss the behavior for each case in the main text. We also illustrate the effect of different input scalings on the adversarial risk in Figures 2.

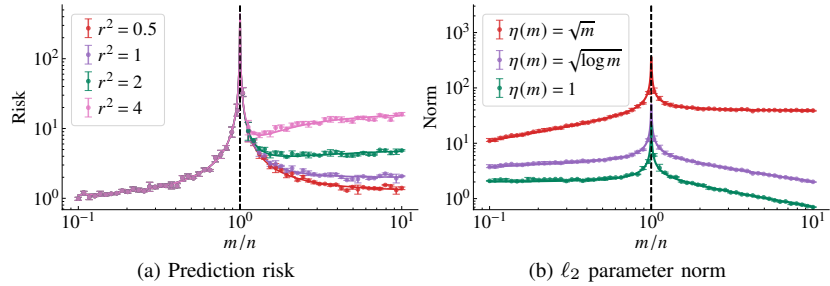


Fig. S.1: **Isotropic features.** In (a), we show the **prediction risk** for $r^2 \in \{0.5, 1, 2, 4\}$. In (b), we show the **parameter norm** for $r^2 = 2$ and for different choices of scaling of the input. The remaining parameters are the same as in Figure 2.

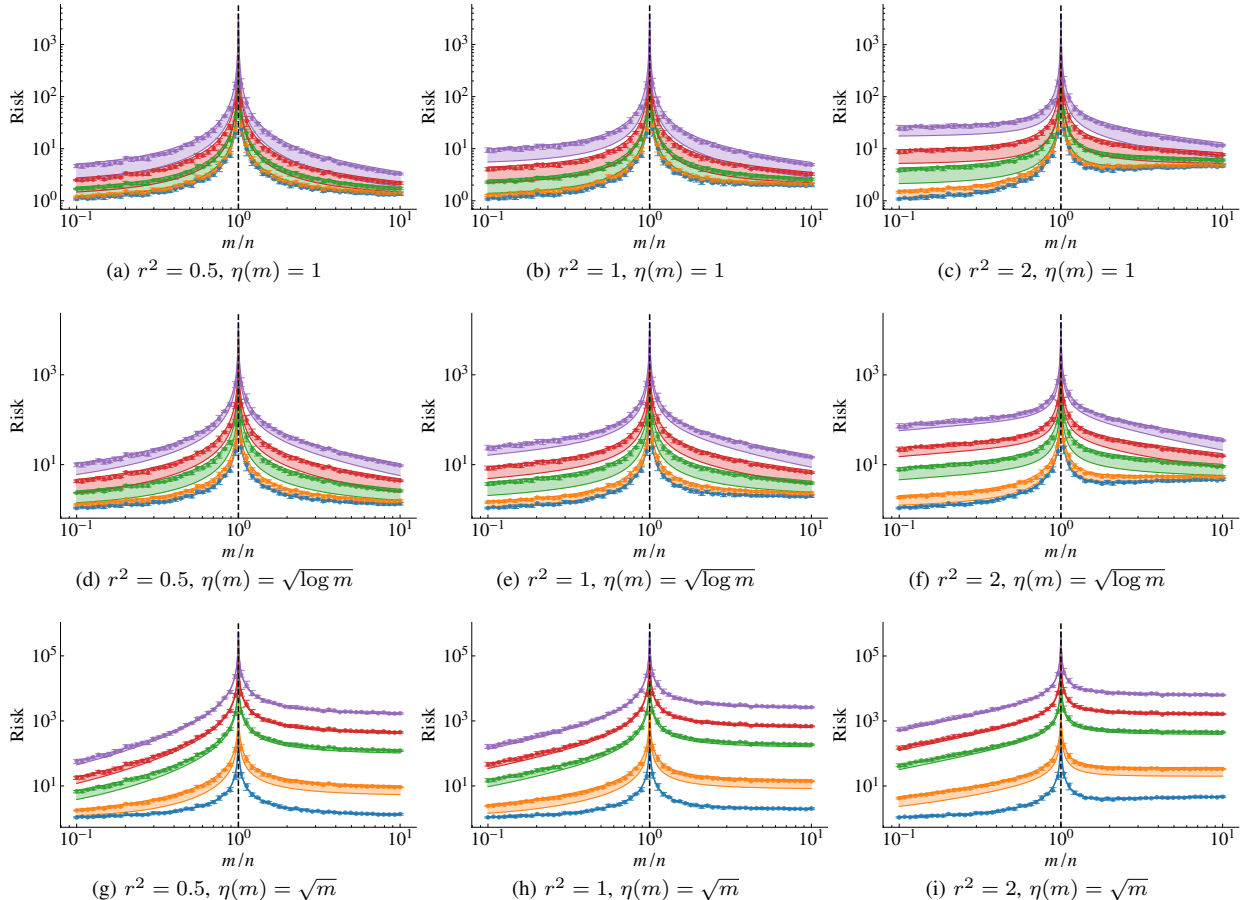


Fig. S.2: **Adversarial ℓ_2 risk, isotropic features.** The setup is the same as in Figure 2 but for a *different scaling* and different values of the parameter norm r^2 .

APPENDIX C
EQUICORRELATED FEATURES MODEL

Here, we consider the case where the features are ρ -equicorrelated. That is, Σ is such that its (i, j) -th entry is:

$$\Sigma_{i,j} = \begin{cases} 1 & i = j, \\ \rho & i \neq j, \end{cases} \quad (\text{S.13})$$

and $x = \Sigma^{1/2}z$ for z composed of i.i.d. features with zero mean, unitary variance, and bounded moments of order greater than 4 that is finite. In this case, the following result holds:

Lemma 14. *Assume that x_i is generated as described above. Also, assume that $\beta \sim \mathcal{N}\left(0, \frac{r^2}{m}I\right)$. Then, as $p, n \rightarrow \infty$ $p/n \rightarrow \gamma$, it holds almost surely that:*

$$\mathbb{E}_\beta[R] \rightarrow \begin{cases} \sigma^2 \frac{\gamma}{1-\gamma}, & \gamma < 1, \\ r^2(1-\rho)(1-\frac{1}{\gamma}) + \sigma^2 \frac{1}{\gamma-1}, & \gamma > 1. \end{cases} \quad (\text{S.14})$$

$$\mathbb{E}_\beta[L_2] \rightarrow \begin{cases} r^2 + \sigma^2 \frac{\gamma}{(1-\gamma)(1-\rho)}, & \gamma < 1, \\ r^2 \frac{1}{\gamma} + \sigma^2 \frac{1}{(\gamma-1)(1-\rho)}, & \gamma > 1. \end{cases} \quad (\text{S.15})$$

The asymptotics for R are presented in Corollary 7 from Hastie *et al.* [7]. The proof for the asymptotics of L_2 follows from Corollary 2 of the same paper and relies on the nice properties of the equicorrelated matrix. The next proposition gives the eigenvalues and eigenvectors of such a matrix. We use $\vec{1}$ to denote a vector of dimension m with all its entries equal to 1. Furthermore, s_i , $i = 1, \dots, n$ denotes the eigenvalues of Σ and v_i the corresponding eigenvectors.

Proposition 15. *Let $\Sigma \in \mathbb{R}^{m \times m}$ be an equicorrelated matrix with its entries defined as in Eq. (S.13). Then $s_1 = 1 + (m-1)\rho$ and $s_i = (1-\rho)$ for every $i \neq 1$. Moreover, $v_1 = \frac{1}{\sqrt{m}}\vec{1}$ and v_i for $i \neq 1$ is such that the sum of its entries is equal to zero, that is, $v_i^\top \vec{1} = 0$.*

Following Hastie *et al.* [7], let us define:

$$\hat{H}_n(s) = \frac{1}{m} \sum_{i=1}^m I\{s \geq s_i\}, \quad (\text{S.16})$$

where I is the indicator function, and is equal to one when $s \geq s_i$ and equal to 0 otherwise. For the equicorrelated matrix, we have that:

$$\hat{H}_n(s) = \frac{m-1}{m} I\{s \geq (1-\rho)\} + \frac{1}{m} I\{s \geq (1 + (m-1)\rho)\}.$$

Hence, $\hat{H}_n(s) \rightarrow H(s) = I\{s \geq 1 - \rho\}$ at all continuity points. Hence, $dH = \delta_{1-\rho}$ and we have $c_0 = \frac{1}{\gamma(\gamma-1)(1-\rho)}$ which when replaced in Corollary 2 establishes the result.³

We illustrate in Figure S.3 empirical experiments and asymptotic results for equicorrelated feature models under ℓ_2 adversarial attacks. In Figure S.4 we illustrate it for ℓ_p attacks when $p \in \{1.5, 2, 20\}$ and in Figure S.5, for $p = \infty$.

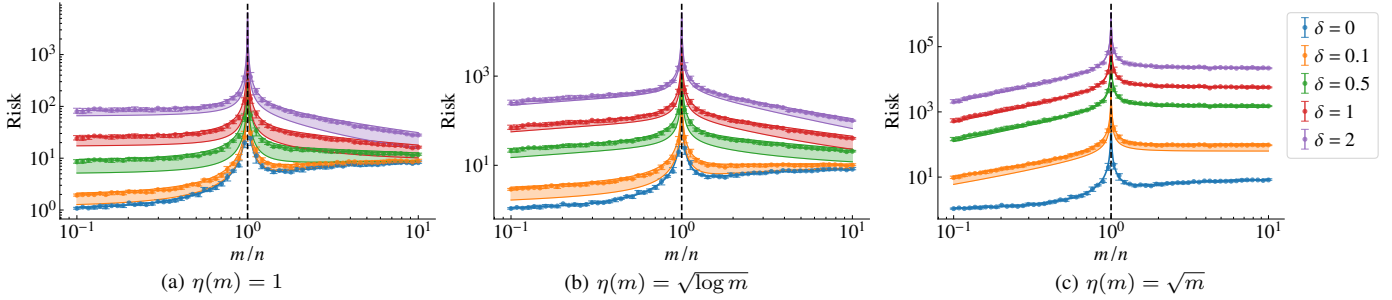


Fig. S.3: Adversarial ℓ_2 risk, equicorrelated features. The solid line show the upper and lower bounds on the asymptotic risk obtained from Lemma 14. The results are for equicorrelated features with $r^2 = 4$, $\sigma^2 = 1$, $\rho = 0.5$. The error bars give the median and the 0.25 and 0.75 quantiles obtained from numerical experiments (10 realizations) with a fixed training dataset of size $n = 300$. We show the results for different scaling choices.

³There is a small typo in Corollary 2 from Hastie *et al.* [7]. The term r^2 should have appeared multiplying the integral for the overparameterized case.

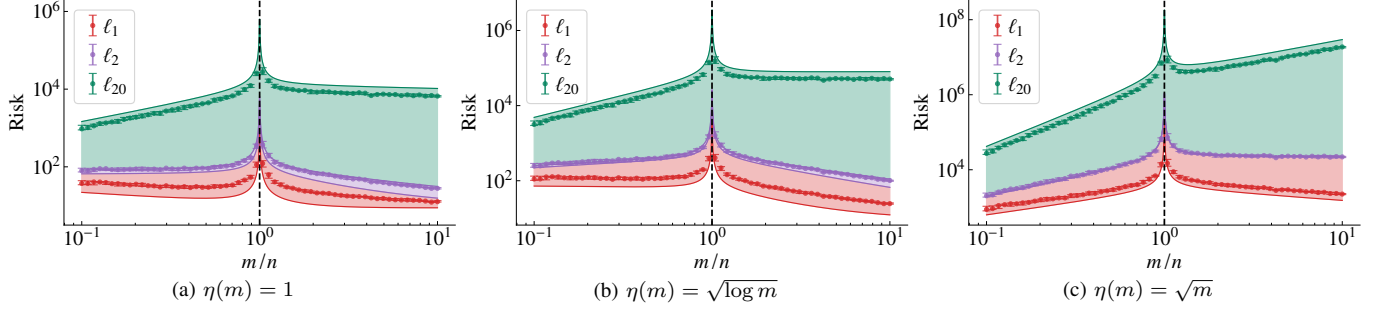


Fig. S.4: **Adversarial ℓ_p risk, equicorrelated features.** The setup is the same as in Figure S.3, but for ℓ_p adversarial attacks, $p \in \{1, 2, \infty\}$ and $\delta = 2$. We show the results for different scaling choices.

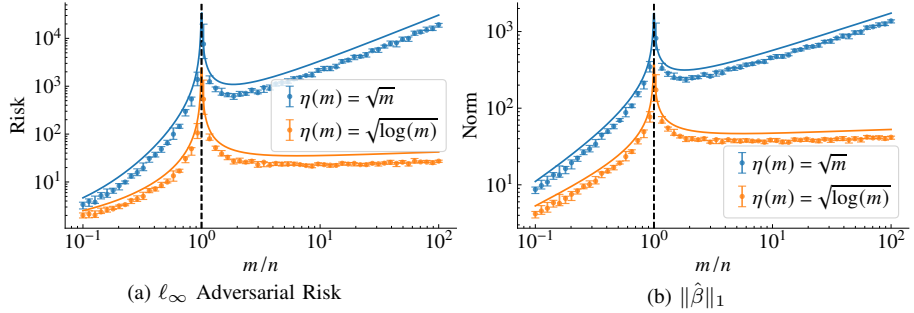


Fig. S.5: **Adversarial ℓ_∞ risk and ℓ_1 parameter norm, equicorrelated features.** The asymptotic upper bound is indicated by the full trace. The error bars give the median and the 0.25 and 0.75 quantiles obtained from numerical experiments (10 realizations). The analysis is performed for a fixed training dataset of size $n = 100$ and for adversarial disturbances of magnitude $\delta = 0.1$. The results are for $r^2 = 1$, $\sigma^2 = 1$, $\rho = 0.5$. We show the results for two different scalings: $\eta(m) = \sqrt{m}$ and $\eta(m) = \sqrt{\log(m)}$.

APPENDIX D LATENT SPACE MODEL

Here we show that the latent model described in Equations (29) and (30) is actually equivalent to a special case of the linear model described in Eq. (11) for the case where the covariates and the noise are both normal, i.e. $x_i \sim \mathcal{N}(0, \Sigma)$ and $\epsilon_i \sim \mathcal{N}(0, \sigma)$. In both formulations, the pair $(x_i, y_i) \in \mathbb{R}^{m+1}$ is jointly a multivariate Gaussian with zero mean. By matching the covariances, we obtain the formulations are equivalent for

$$\begin{aligned} \beta &= W(I_d + W^\top W)^{-1}\theta, \\ \Sigma &= I_p + WW^\top, \\ \sigma^2 &= \sigma_\xi^2 + \theta^\top(I_d + W^\top W)^{-1}\theta. \end{aligned} \tag{S.17}$$

That is, from Eq. (11) the covariance matrix of the joint Gaussian vector $(x_i, y_i) \in \mathbb{R}^{m+1}$ is:

$$\begin{bmatrix} \mathbb{E}[x_i x_i^\top] & \mathbb{E}[y_i x_i^\top] \\ \mathbb{E}[y_i x_i^\top] & \mathbb{E}[y_i y_i^\top] \end{bmatrix} = \begin{bmatrix} \Sigma & \beta^\top \Sigma \\ \Sigma \beta & \beta^\top \Sigma \beta + \sigma^2 \end{bmatrix}. \tag{S.18}$$

On the other hand, the latent model (29) and (30) implies the following covariance matrix for this same vector

$$\begin{bmatrix} \mathbb{E}[W z_i z_i^\top W^\top + u_i u_i^\top] & \mathbb{E}[\theta^\top z_i z_i^\top W + \xi_i u_i^\top] \\ \mathbb{E}[\theta^\top z_i z_i^\top W + \xi_i u_i^\top] & \mathbb{E}[\theta^\top z_i z_i^\top \theta + \xi_i \xi_i^\top] \end{bmatrix} = \begin{bmatrix} WW^\top + I_d & \theta^\top W^\top \\ W\theta & \theta^\top \theta + \sigma_\xi^2 \end{bmatrix}. \tag{S.19}$$

Using the matrix inversion lemma $(I_d + W^\top W)^{-1} = I_d + W^\top(I - WW^\top)^{-1}W$ and the identity $(I_d + W^\top W)^{-1}W^\top = W(I_d + WW^\top)^{-1}$ it is easy to check that (S.17) renders the two covariance matrices to be equal and the two data generation procedures equivalent.

Now, the hypothesis that $W^\top W = m/dI_d$ makes the calculation of the asymptotics easy. First notice that: $\|\beta\|_2^2 = \beta^\top \beta = \theta^\top(I_d + W^\top W)^{-1}W^\top W(I_d + W^\top W)^{-1}\theta$ using the fact that $W^\top W = m/dI_d$ we obtain: $\|\beta\|_2^2 = \frac{m/d}{(1+m/d)^2} \|\theta\|_2^2$.

Moreover, it is quite straight forward to compute the eigenvalues and eigenvectors of $\Sigma = WW^\top + I_p$. From the hypothesis, it follows that $\Sigma W = (1 + m/d)W$. Hence, the first d eigenvectors v_i are the columns of $\sqrt{d/m}W$ and the first d eigenvalues

are equal to $s_i = (1 + m/d)$. Now the remaining eigenvectors are vectors orthogonal to the columns of W such that $W^T v_i = 0$ for $i > d$. The corresponding eigenvalues would be $s_i = 1$.

Following Hastie *et al.* [7], let us define:

$$\widehat{H}(s) = \frac{1}{m} \sum_{i=1}^m I\{s \geq s_i\}, \quad \widehat{G}(s) = \frac{1}{\|\beta\|_2^2} \sum_{i=1}^m (\beta^T v_i)^2 I\{s \geq s_i\}, \quad (\text{S.20})$$

Hence:

$$\widehat{H}(s) = \frac{d}{m} I\{s \geq (1 + m/d)\} + \left(1 - \frac{d}{m}\right) I\{s \geq 1\}. \quad (\text{S.21})$$

Moreover, $v_i^T \beta = 0$ if $i > d$, i.e., β is orthogonal to the last $m - d$ eigenvectors. Hence, simple manipulation yields that:

$$\widehat{G}(s) = \frac{d/m \|W^T \beta\|_2^2}{\|\beta\|_2^2} I\{s \geq (1 + m/d)\} = I\{s \geq (1 + m/d)\}. \quad (\text{S.22})$$

Let us define $\psi = \frac{d}{m}$.

Proposition 16. *Let $c_0 = c_0(\psi, \gamma)$ be the unique non-negative solution of the following second-order equation:*

$$1 - \frac{1}{\gamma} = \frac{1 - \psi}{1 + c_0 \gamma} + \frac{\psi}{1 + c_0 (1 + \psi^{-1}) \gamma}. \quad (\text{S.23})$$

And define:⁴

$$\begin{aligned} \mathcal{B}(\psi, \gamma) &= \left\{ 1 + \gamma c_0 \frac{\mathcal{E}_1(\psi, \gamma)}{\mathcal{E}_2(\psi, \gamma)} \right\} \cdot \frac{(1 + \psi^{-1})}{(1 + c_0 \gamma (1 + \psi^{-1}))^2}, \\ \mathcal{V}(\psi, \gamma) &= \gamma c_0 \frac{\mathcal{E}_1(\psi, \gamma)}{\mathcal{E}_2(\psi, \gamma)}, \\ \mathcal{E}_1(\psi, \gamma) &= \frac{1 - \psi}{(1 + c_0 \gamma)^2} + \frac{\psi (1 + \psi^{-1})^2}{(1 + c_0 \gamma)^2}, \\ \mathcal{E}_2(\psi, \gamma) &= \frac{1 - \psi}{(1 + c_0 \gamma)^2} + \frac{1 + \psi}{(1 + c_0 (1 + \psi^{-1}) \gamma)^2}, \end{aligned} \quad (\text{S.24})$$

then:

$$R \rightarrow \begin{cases} \sigma^2 \frac{\gamma}{1-\gamma}, & \gamma < 1, \\ r^2 \mathcal{B}(\psi, \gamma) + \sigma^2 \mathcal{V}(\psi, \gamma), & \gamma > 1. \end{cases} \quad (\text{S.25})$$

$$L_2 \rightarrow \begin{cases} r^2 + \sigma^2 \frac{\gamma}{(1-\gamma)(1+\psi)}, & \gamma < 1, \\ r^2 \frac{c_0 \gamma (1 + \psi^{-1})}{1 + c_0 \gamma (1 + \psi^{-1})} + \sigma^2 c_0 \gamma, & \gamma > 1. \end{cases} \quad (\text{S.26})$$

The proposition is (partially) provided by Hastie *et al.* [7, Corollary 4] and extended here to also state the asymptotic for L_2 and for R in the underparameterized region, both results actually follow from the developments in [7]. In the overparameterized region, the proof follows from replacing \widehat{G} and \widehat{H} from Eq. (S.21) and Eq. (S.22) in Definition 1 from Hastie *et al.* [7] and from further simplifying the expressions. It then follows from the (more general) Theorem 2 in [7] that $R \rightarrow r^2 \mathcal{B}(\psi, \gamma) + \sigma^2 \mathcal{V}(\psi, \gamma)$. In the underparameterized region, the result can be obtained using Theorem 1 in [7]. The convergence of the L_2 follows from similar analysis using Corollary 3 in [7].

⁴We define $\mathcal{B}(\psi, \gamma)$ and $\mathcal{V}(\psi, \gamma)$ slightly different from [7]. The reason is to make explicit the role of r^2 and σ^2 . The formulas are equivalent.

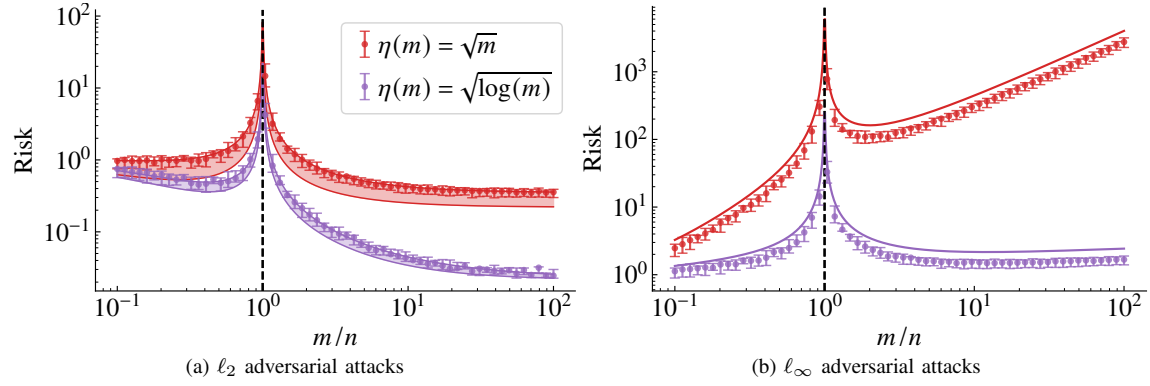


Fig. S.6: **Adversarial ℓ_p risk, latent space model.** The setup is the same as in Figure 6, but we plot the asymptotics obtained from the above proposition. In (a), we show the upper and lower bounds; in (b), we show only the upper bound. The argument why the upper bound is followed closely for ℓ_∞ adversarial attacks is provided in the main text.

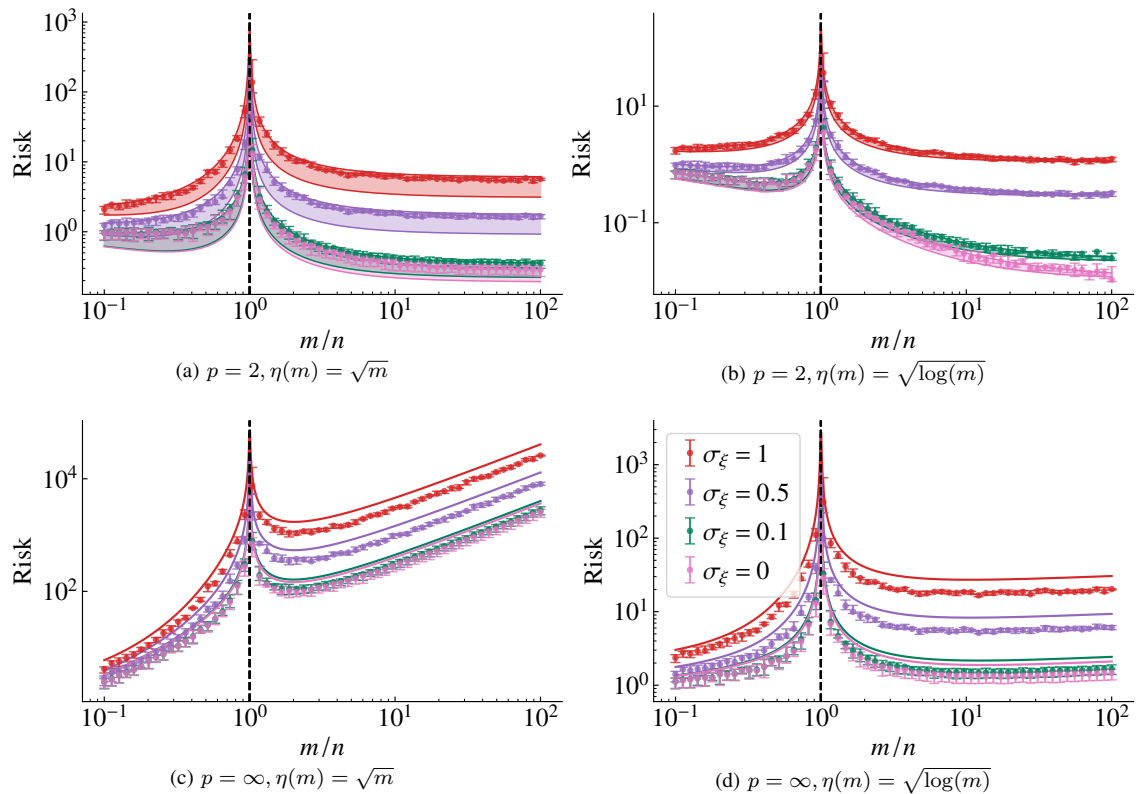


Fig. S.7: **Adversarial risk, latent space model, different values of σ_ξ .** The setup is the same as in Figure S.6 but for different values of noise σ_ξ .

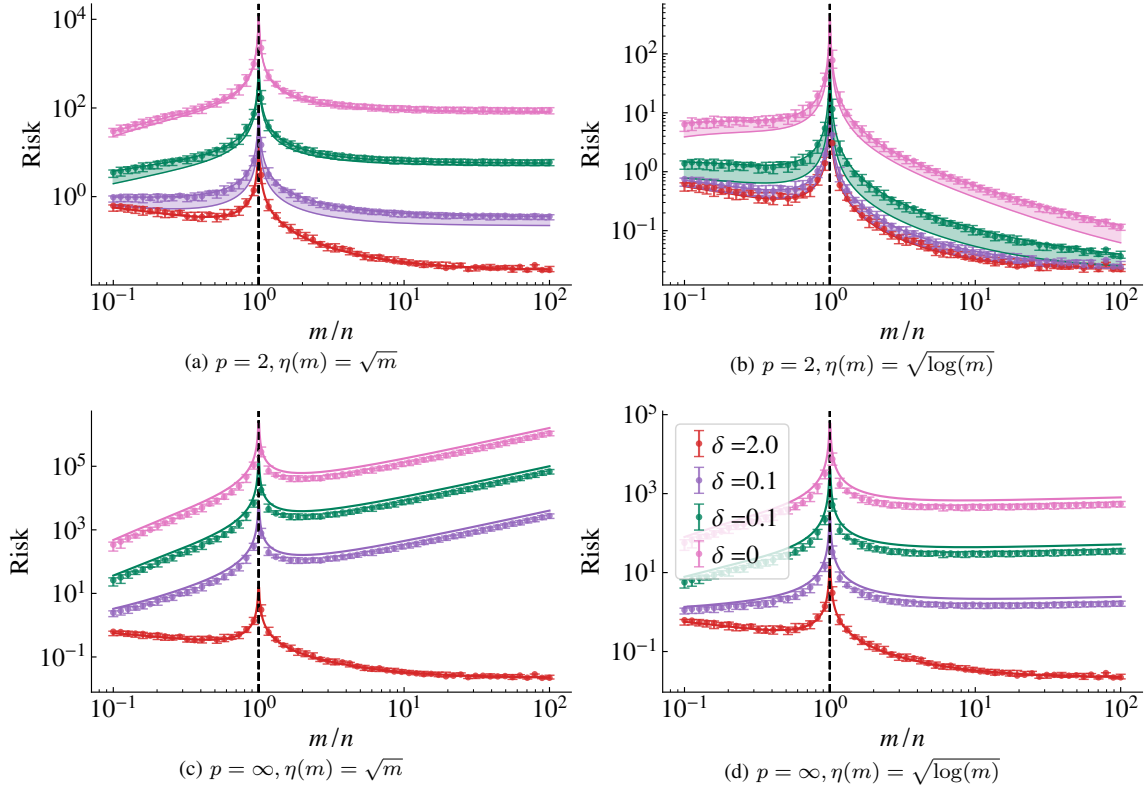


Fig. S.8: **Adversarial risk, latent space model, different δ .** The setup is the same as in Figure S.6 but for different values of δ . Here $\delta = 0$ correspond to no adversarial attack.

APPENDIX E COMPARISON BETWEEN REGULARIZATION METHODS IN ISOTROPIC FEATURES MODEL

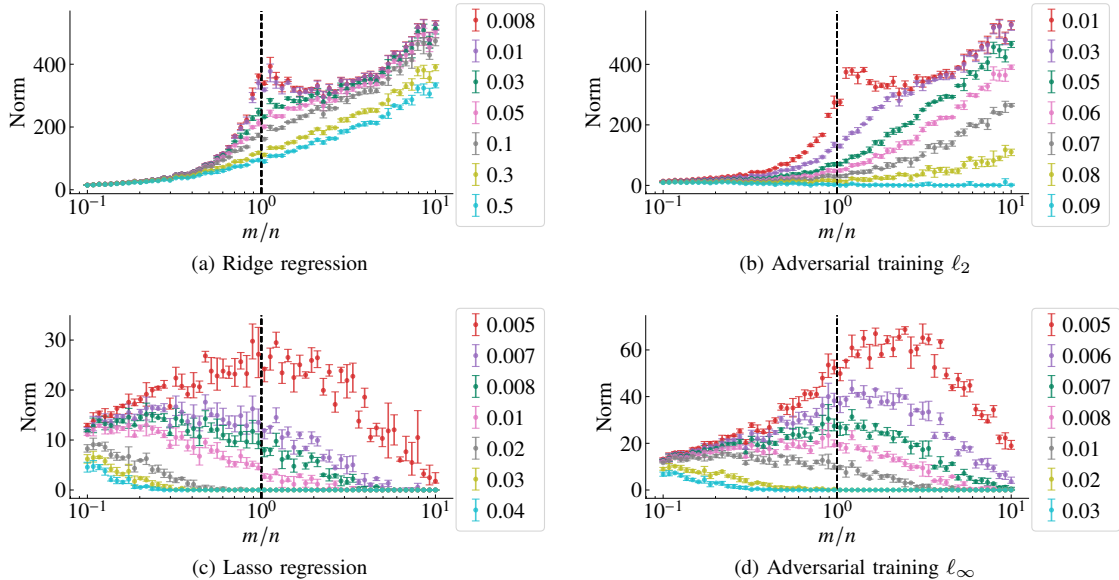


Fig. S.9: **Parameter norm $\|\beta\|_1$.** The input variables are scaled with $\eta(m) = \sqrt{m}$. The error bars give the median and the 0.25 and 0.75 quantiles obtained from the numerical experiment (4 realizations) for a fixed training dataset of size $n = 100$. The values of δ for each experiment are indicated in the plot. We repeat the experiment for different amounts of regularization. The regularization parameter δ defined in Eq. (31) for the adversarial training and in Eq. (32) and (33) for ridge regression and lasso. It is indicated in the plot by the different colors.

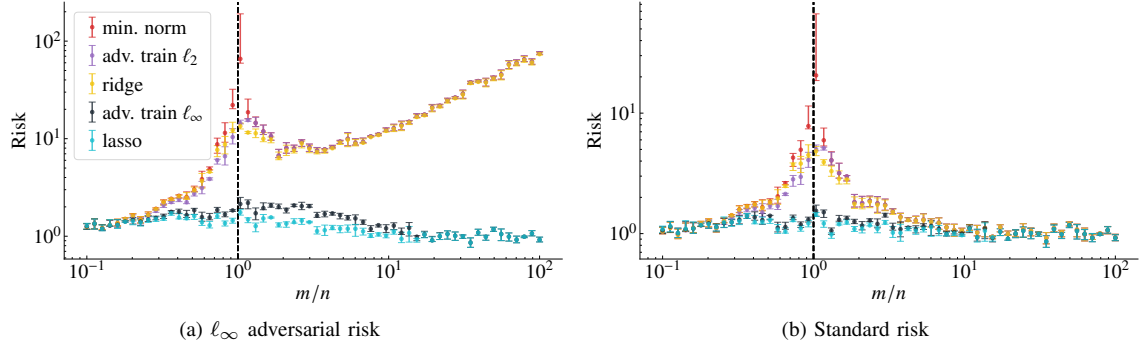


Fig. S.10: **Adversarial ℓ_∞ risk.** On the y -axis we show the risk for models obtained by different training methods. In (a), it is the ℓ_∞ adversarial risk; and, in (b) the standard risk. On the x -axis we have the ratio between the number of features m and the number of training datapoints n . The error bars give the median and the 0.25 and 0.75 quantiles obtained from numerical experiment (4 realizations). We use $\delta = 0.01$ during both inference (to compute the adversarial risk) and adversarial training, as in Eq. (31). We also use $\delta = 0.01$ for lasso and ridge regression, see Eq. (32) and (33).